Journal of Zhejiang University-SCIENCE B (Biomedicine & Biotechnology) in press

www.jzus.zju.edu.cn; www.springer.com/journal/11585

E-mail: jzus_b@zju.edu.cn

Review

https://doi.org/10.1631/jzus.B2500786

Blood-brain barrier permeability assessment: from biomimetic models to multimodal imaging

Miaomiao WANG[1], Lu GAN[1], Yiru FAN[1], Chenxi DUAN[2,3], Ying ZHU[1], Shihua LUO[4]✉, Yanhong SUN[1]✉

[1] *Institute of Materiobiology, College of Sciences, Shanghai University, Shanghai 200444, China*
[2] *Shanghai Institute of Applied Physics, Chinese Academy of Sciences, Shanghai 201800, China*
[3] *University of Chinese Academy of Sciences, Beijing 100049, China*
[4] *Department of Traumatology, Rui Jin Hospital, School of Medicine, Shanghai Jiao Tong University, Shanghai 200025, China*

Abstract: The blood-brain barrier (BBB) is a vital physiological structure that maintains the microenvironmental homeostasis in the central nervous system (CNS). Imbalances in its permeability play a key role in various neurological disorders, including stroke, neurodegenerative diseases, and brain tumors. The development of precise techniques for assessing BBB permeability is therefore paramount for elucidating the mechanisms of neurological diseases, overcoming drug development challenges and achieving precise diagnosis and treatment of CNS disorders. This review systematically summarizes the latest advances in the assessment of BBB permeability. Regarding *in vitro* models, platforms have evolved from the traditional Transwell system to microfluidic chips incorporating fluid shear forces, and subsequently to highly biomimetic brain organoids, with continuous improvements in the ability to simulate the neurovascular unit (NVU) microenvironment. For *in vivo* assessment, we detail the principles and applications of imaging techniques, including dynamic contrast-enhanced magnetic resonance imaging (DCE-MRI), positron emission tomography (PET), second near-infrared (NIR-II) fluorescence imaging, and two-photon microscopy (TPM), highlighting their complementary strengths in macroscopic quantification, molecular targeting, and microscopic dynamic observation. The integration of multi-modal technologies and precise quantitative assessment is a prominent trend. Future investigations will focus on artificial intelligence (AI)-driven personalized permeability assessment, the development of novel intelligent probes, and the dynamic real-time monitoring of the BBB, thereby providing powerful methodological support for neurological disease research.

Key words: Blood brain barrier; Permeability assessment; *In vitro* blood brain barrier model; *In vivo* imaging; Central nervous system

1 Introduction

The blood-brain barrier (BBB) is a highly selective, semi-permeable structure that separates the blood circulatory system and the central nervous system (CNS). It meticulously regulates the exchange of substances, thereby playing a crucial role in maintaining the homeostasis of the cerebral microenvironment (He et al., 2018; Wu et al., 2023; Liu et al., 2025). The BBB primarily comprises endothelial cells, astrocytes, pericytes, and the

✉ Shihua LUO, jqab@163.cm
✉ Yanhong SUN, sunyanhong@shu.edu.cn
Miaomiao WANG, https://orcid.org/0009-0007-3819-9958
Shihua LUO, https://orcid.org/0009-0008-0862-5132
Yanhong SUN, https://orcid.org/0000-0002-1774-8598

Received Dec. 1, 2025; Revision accepted Mar. 12, 2026;
Crosschecked xxx. xx, 20xx; Published online xxx. xx, 20xx

basement membrane (Fig. 1). Brain microvascular endothelial cells (BMECs) constitute the core component of the BBB, forming a continuous physical barrier through intercellular connections, primarily tight junctions and adherens junctions. Tight junctions, composed of transmembrane proteins linked to the actin cytoskeleton via cytoplasmic scaffolding proteins, are responsible for maintaining selective permeability and controlling tissue homeostasis (Anderson and Van Itallie, 2009; Luissint et al., 2012; Dong, 2018; Ahlawat et al., 2020). Adherens junctions, primarily constituted by vascular endothelial cadherin (VE-cadherin) and its intracellular binding partners, such as β-catenin, are instrumental in regulating intercellular adhesion strength and barrier integrity (Vorbrodt and Dobrogowska, 2003; Turowski and Kenny, 2015; Stamatovic et al., 2016; Malinova and Huveneers, 2018). Studies have shown that the downregulation or dysfunction of these junctional proteins can lead to aberrant BBB permeability, contributing to the pathogenesis of various neurological disorders (Krol et al., 2013). Astrocytes envelop the cerebral microvasculature with their endfeet. By secreting diverse signaling molecules, they induce tight junction formation among endothelial cells and maintain barrier properties (Zhao et al., 2015; Schurhoff and Toborek, 2023). Pericytes, embedded within the capillary basement membrane, ensheathe the endothelial cells. They are not only capable of modulating capillary blood flow by contracting but also participate in the development, homeostatic maintenance, and repair of barrier function (Bell et al., 2010; Kisler et al., 2017; Kadry et al., 2020). The basement membrane, a dense extracellular matrix network, provides structural support for the BBB's cellular components and mediates cell–matrix interactions to regulate its permeability (Bayir et al., 2019).

As a physiological interface, the BBB allows the passage of water and certain small molecules while effectively excluding the majority of large-molecular-weight substances. This selective impermeability shields the CNS from toxins, pathogens, and metabolic waste present in the systemic circulation, while also restricting the nonspecific permeation of neurotransmitters and hormones, providing a highly stable internal environment for neuronal activity (Bhattacharya et al., 2020; Segarra et al., 2021). For instance, specific ion channels and transport proteins expressed at the BBB meticulously regulate ion flux between the blood and brain tissue (Harilal et al., 2020; Yang et al., 2020). This precise control maintains ionic balance and pH homeostasis between the blood and cerebrospinal fluid, ensuring an optimal cerebral microenvironment. Furthermore, the BBB actively facilitates the delivery of essential nutrients to the brain via specialized transport proteins to meet its high metabolic demands. For example, the GLUT1 transporter is responsible for the efficient translocation of glucose—the brain's primary energy source—from the blood into the CNS. Similarly, the LAT1 transporter mediates the uptake of large neutral amino acids (De Vivo et al., 1991). In terms of active defense, the BBB expresses a repertoire of efflux transporters, including P-glycoprotein (P-gp) and breast cancer resistance protein (BCRP), which can effectively pump xenobiotics and metabolic byproducts back into the bloodstream, thereby preventing the accumulation of potentially harmful substances within the brain (Balzer et al., 2022). Recent studies have further elucidated the BBB's role in the glymphatic system, a paravascular pathway responsible for cerebrospinal and interstitial fluid circulation. This process, enabled by aquaporin-4 (AQP4) water channels on astrocytic endfeet, promotes the convective flow of cerebrospinal fluid through the brain parenchyma and facilitates interstitial solute clearance. This mechanism is recognized as essential for maintaining a clean internal cerebral environment (Iliff et al., 2012).

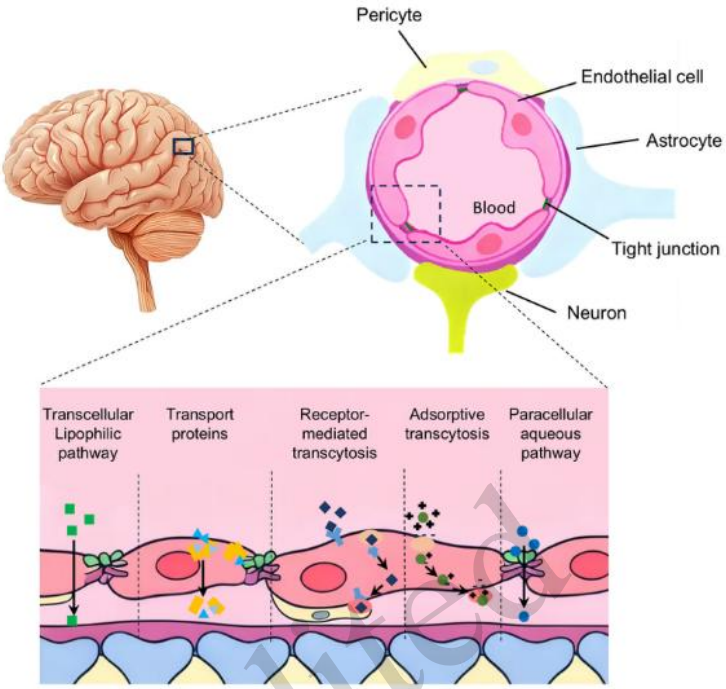

Fig. 1 Schematic of blood-brain barrier (BBB) structure and key transport pathways. The BBB comprises endothelial cells interconnected with tight junctions, and is supported by pericytes and astrocytic endfeet. The schematic highlights the principal pathways of substance traversal: the transcellular route (including lipophilic diffusion and transcytosis) and the restricted paracellular aqueous pathway.

The selective permeability of the BBB is not only a fundamental physiological requirement for CNS homeostasis but is also a critical determinant in the pathogenesis and therapeutic management of various CNS disorders. Numerous studies have demonstrated that BBB dysfunction represents a central pathological event in many neurological diseases. For instance, amyloid-β (Aβ) is a primary pathological protein in Alzheimer's disease (AD). The production and deposition of Aβ are key factors influencing the progression and prognosis of AD, and this process is closely related to the BBB's diminished capacity to clear Aβ. Furthermore, Aβ deposition can damage the structure of the BBB, establishing a vicious cycle of "Aβ deposition—BBB impairment—attenuated clearance ability—further Aβ accumulation," thereby accelerating disease progression (Wang et al., 2021). Consequently, in addition to their role in the pathogenesis of CNS diseases, changes in BBB permeability can serve as diagnostic indicators and prognostic biomarkers for associated disorders. BBB permeability is also a pivotal factor in drug development, affecting the therapeutic efficacy of interventions for CNS diseases. While an intact BBB effectively restricts the entry of most blood-borne substances into the brain, it also hinders the delivery of most therapeutic agents. It is estimated that over 98% of small-molecule drugs and nearly all large-molecule biologics fail to cross the BBB and reach brain tissue in therapeutically relevant concentrations, presenting a major bottleneck in the treatment of diseases such as stroke, neurodegenerative diseases, brain tumors, meningitis, and multiple sclerosis (Banks, 2016; Pandit et al., 2020). Therefore, advanced techniques for assessing BBB permeability are crucial for the early-stage screening of candidate compounds with favorable brain-penetration potential, thereby enhancing the success rate and efficiency of CNS-targeted drug development programs.

The development of robust methodologies for assessing BBB permeability is of paramount importance for elucidating the mechanisms underlying CNS pathologies and for promoting the discovery of therapeutic agents.

A series of significant breakthroughs in detection technologies has been made in recent years, ranging from *in vitro* models to *in vivo* imaging, providing powerful tools for improving understanding of the BBB's function and regulatory mechanisms. This review systematically summarizes recent progress in this field and compares and analyzes the advantages, limitations, and suitable application scenarios of various technologies. It aims to provide valuable methodological references and conceptual frameworks for research on the structural and functional aspects of the BBB, the mechanisms underlying CNS disorders, and therapeutic strategies.

2 *In vitro* assessments of BBB permeability

2.1 *In vitro* BBB model

The construction of *in vitro* BBB models that accurately simulate the physiological parameters and molecular characteristics of the neurovascular unit (NVU) provides a pivotal tool for analyzing the pathological mechanisms and screening of potential therapeutic drugs for CNS diseases. Driven by technologies such as microfluidics and organoids, the field of *in vitro* BBB models has recently undergone significant innovation. This has led to a transition from traditional monolayer, two-dimensional co-culture systems toward three-dimensional (3D) biomimetic systems that more closely simulate the *in vivo* microenvironment (Sivandzade and Cucullo, 2018). Presently, there are two main types of *in vitro* models for detecting BBB permeability: static models based on Transwell chambers and dynamic models (Table 1).

2.1.1 Static BBB model

The static model is the most widely used *in vitro* BBB model. It is constructed by incubating BMECs onto the porous membrane of a Transwell insert. The apparent permeability coefficient (P_{app}) is calculated by measuring the translocation of test substances from the apical (luminal) compartment to the basolateral compartment, thereby evaluating barrier permeability. Based on the cellular composition, static BBB models are further classified into two principal categories: monoculture and co-culture systems (Fig. 2) (Bagchi et al., 2019). The monoculture model, in its most fundamental form, initially used primary BMECs isolated from species such as rats, cows, or pigs. A key advantage of these primary cultures is their retention of critical BBB characteristics, including well-defined tight junctions and the polarized expression of various transporters (Cecchelli et al., 2007). To circumvent the limitations of primary cells—namely, low yield and susceptibility to contamination—immortalized cell lines (e.g., hCMEC/D3) have been widely adopted (Muruganandam et al., 1997; Weksler et al., 2013). However, these cell lines often exhibit an incomplete barrier phenotype, frequently necessitating functional enhancement with compounds such as cAMP or glucocorticoids to improve barrier properties (Hurst and Fritz, 1996; Franke et al., 1999; Ogunshola, 2011; Naik and Cucullo, 2012; Daniels et al., 2013). The monoculture model is simple to operate and well-suited for high-throughput drug screening and basic mechanistic studies, but its fundamental limitations lie in the absence of synergistic interactions with other cells in the NVU and in its inability to simulate hemodynamic shear stress. Consequently, it falls short of fully recapitulating the complex functionality of the *in vivo* BBB (Mantecón-Oria et al., 2022a). To compensate for the shortcomings of monoculture systems, co-culture models have been developed. Co-culturing BMECs with astrocytes has been shown to promote tight junction maturation and reduce pinocytosis activity (Rubin et al., 1991; Dohgu et al., 2005). Further introduction of pericytes into a triple-culture model enables secretion of factors such as TGF-β, which synergistically increase transendothelial electrical resistance (TEER), lower passive permeability, and enhance efflux transporter activity. It is currently regarded as the static model that most closely approximates the *in vivo* BBB (Nakagawa et al., 2009).

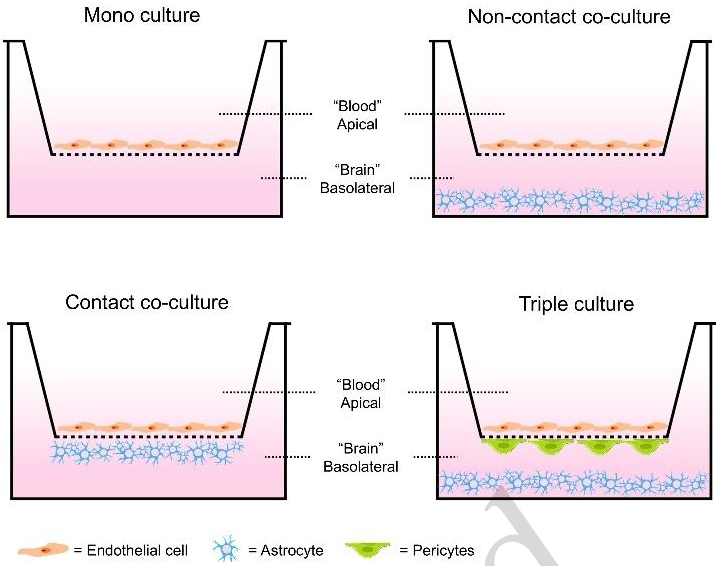

Fig. 2 Schematic of four common static *in vitro* models of the BBB. These Transwell-based models vary in cellular complexity. Mono-culture consists of only brain microvascular endothelial cells (BMECs). Co-culture models consist of BMECs and astrocytes. In the non-contact co-culture model, BMECs are seeded on the Transwell membrane while astrocytes are cultured in the basolateral compartment, allowing paracrine signaling. In the contact co-culture model, BMECs are grown in direct physical contact with an astrocyte layer. In the triple culture model, BMECs are co-cultured with both astrocytes and pericytes, thereby best recapitulating the native neurovascular unit. The apical chamber represents the "blood" side, and the basolateral chamber represents the "brain" side.

2.1.2 Dynamic BBB model

The dynamic model can more realistically simulate the mechanical microenvironment of the BBB *in vivo* by introducing fluid shear stress (Fig. 3). Application of shear stress has been shown to upregulate the expression of tight junction proteins, such as ZO-1, and thereby enhance barrier integrity (Bagchi et al., 2019). Representative dynamic BBB platforms include the cone-plate BBB apparatus (Naik and Cucullo, 2012), hollow fiber bioreactors (Stanness et al., 1997; Janigro et al., 1999; Cucullo et al., 2008; Nogueira et al., 2021), microfluidics (Jiang et al., 2019; Oddo et al., 2019; Wang et al., 2020; Hajal et al., 2022), and organoids (Bergmann et al., 2018; Logan et al., 2019; Dao et al., 2024). The cone-plate BBB apparatus uses a rotating cone to impose a defined shear stress on endothelial cells, facilitating the study of their mechanoresponse. However, its utility in modeling the BBB is limited by its inherent inability to incorporate the multicellular crosstalk essential for a fully functional NVU. In contrast, hollow fiber bioreactors feature a 3D tubular configuration in which BMECs are seeded onto the luminal surface of semi-permeable hollow fibers. Culture medium is perfused through the fiber lumen, generating physiological shear stress, while astrocytes or pericytes can be co-cultured within the extracapillary space (Cucullo et al., 2011). This 3D tubular architecture significantly extends the viable culture period of the model (from days to months) and induces cells to form *in vivo*-like morphologies and more complex connections (Neuhaus et al., 2006).

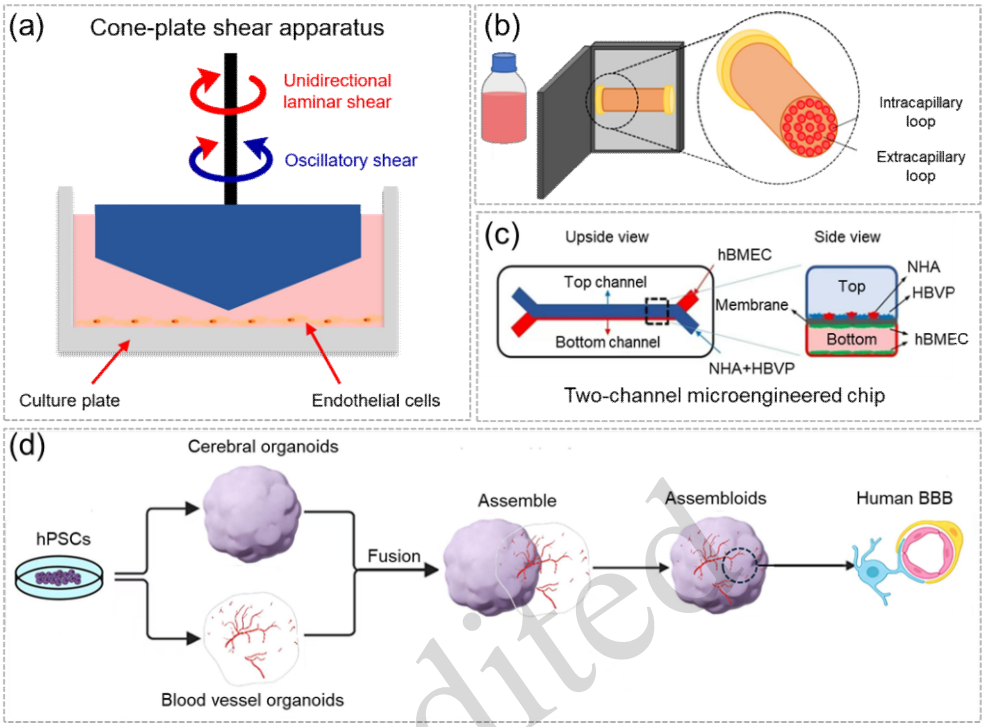

Fig. 3 Dynamic BBB model. (a) Cone-plate BBB apparatus. (b) Schematics of a hollow fiber bioreactor system and a close-up of the hollow fiber module, comprising an outer sheath and internal fibers. Cells can adhere to the fiber surface, enabling mass transfer through the semipermeable membrane. Reprinted from Nogueira et al. (2021), Copyright (2021), with permission from MDPI. (c) A two-channel micro-engineered chip had human brain microvascular endothelial cells (hBMECs, green) on all surfaces of the bottom channel, and normal human astrocytes (NHAs, red) and human brain vascular pericytes (HBVPs, blue) on the surface of the top channel. Reprinted from Yang et al. (2024), Copyright (2024), with permission from MDPI. (d) Schematic protocol for generating 3D human BBB assembloids from cerebral organoids and blood vessel organoids.

Over recent years, dynamic model technologies have evolved to construct more complex and physiologically relevant systems that more closely approximate human physiology, with the aim of enhancing their predictive value (Banerjee et al., 2016; Bhalerao et al., 2020; Mantecón-Oria et al., 2020). For instance, polycaprolactone/graphene (PCL/G) composite materials have been explored to promote astrocyte differentiation (Mantecón-Oria et al., 2022b), and the development of transparent polyvinylidene fluoride (PVDF) hollow fibers has successfully addressed the critical bottleneck that traditional models could not overcome: enabling the real-time, non-invasive observation of cells (Mantecón-Oria et al., 2025). However, hollow fiber models still face inherent challenges on the path toward achieving higher levels of biomimetic realism. Their relatively simple tubular structure struggles to mimic the complex tissue configurations found *in vivo*, and their control over fluid dynamics remains rudimentary, making it difficult to accurately reproduce physiological shear forces and pulsatile flow fields. In contrast, microfluidic technology, distinguished by its high integration capacity, controllable fluidic environment, and ability to construct 3D architectures, has emerged as a cutting-edge research focus (Mármol et al., 2023; Ceccarelli et al., 2024; Sun and Song, 2024; Sonninen et al., 2025). A typical design incorporates parallel channels for the co-culture of endothelial cells, pericytes, and astrocytes, which can be utilized to investigate the trans-barrier transport mechanisms of

nanoparticles or antibodies, such as those targeting the transferrin receptor (Wevers et al., 2018). More advanced systems enable the fabrication of 3D tubular vascular structures within the chip. These systems have been successfully employed to quantitatively assess the permeability of cell-penetrating peptides, including ApoE, which undergo transport mediated by the LRP1 receptor. Furthermore, they enable precise determination of the apparent permeability coefficient of drugs through LC-MS/MS analysis, with the generated data exhibiting consistent trends with *in vivo* studies. This demonstrates significant potential for substituting animal experiments during early-stage drug development (Chung et al., 2020; Yang et al., 2024). Despite these advantages, microfluidic models have yet to fully replicate the multicellular interactions, dynamic blood flow, and long-term stability of the native BBB, owing to limitations in structural complexity and physiological realism.

Organoids are another rapidly developing type of BBB model. They are widely applied in drug delivery and disease modeling due to their highly biomimetic characteristics. The principal advantage of this type of model is the ability to precisely simulate the *in vivo* microenvironment and spatial architecture of the BBB, a key challenge for traditional microfluidics. For instance, Nzou et al. developed a 3D human cortical spheroid BBB model incorporating six major brain cell types, including endothelial cells, pericytes, and astrocytes, with tight junctions and charge selectivity (Nzou et al., 2018). Studies using this model demonstrate its utility for neurotoxicity screening and hypoxic disease modeling, providing a more human-relevant *in vitro* platform for drug development and neurological disease research. To address the challenges of throughput and reproducibility in organoid models, Simonneau et al. engineered a high-throughput BBB organoid platform based on a hydrogel microwell array (Simonneau et al., 2021). By co-culturing the three core cell types, their system enables the simultaneous generation of thousands of uniform organoids in a single experiment, coupled with a semi-automated imaging and analysis pipeline. Notably, this study pioneered the application of CRISPR/Cas9 gene-editing technology within this platform to successfully elucidate the molecular mechanisms governing the BBB penetration of specific antibodies. This integrated technological framework provides an efficient and robust tool for the large-scale screening of CNS-targeting antibodies and the systematic analysis of their translocation mechanisms.

Although 3D structures more accurately reflect the BBB environment in the human body, they face challenges, including a lack of standardized protocols and the limited maturity and long-term stability of the barriers. Overcoming these obstacles will likely require a synergistic strategy that combines the controllability of microfluidics with the biological authenticity of organoids, paving the way for transformative advances in CNS drug development and disease modeling.

Table 1 Comparison of *in vitro* BBB models

In vitro model		Cell composition	Physiological functions and characteristics	Physiological fidelity	Primary application scenarios
Static model	Mono culture	Endothelial cell	Reflects basic barrier properties Low TEER	Low	Study of signaling pathways, transporter kinetics, binding affinity, and high-throughput screenings
	Co-culture	Endothelial cell Astrocytes Pericytes	Enables partial biochemical signal responses through fluid exchange Improved TEER	Medium	Standard permeability assays and mechanistic studies.
Dynamic model	Cone-plate BBB apparatus	Endothelial cells (expandable to co-culture)	Applies controlled shear stress TEER can be modulated	Medium	Hemodynamic study
	Hollow fiber bioreactors	Endothelial cells astrocytes/pericytes (3D co-culture)	Dynamic perfusion provides shear stress, supports sustained high barrier function, and allows for long-term responsiveness to circulating factors/drugs.	High	Validation and optimization of lead compounds in drug discovery
	Microfluidics (BBB-on-a-Chip)	Endothelial cells Astrocytes, Pericyte Other NVU) cells (controllable 3D co-culture)	Highly controllable system capable of integrating shear force, chemical gradients, and real-time monitoring.	High	High spatiotemporal resolution research on mechanisms, drug evaluation and disease modeling.
	Brain organoids	Endothelial cells, pericytes, astrocytes, neurons, microglia. Self-organized or engineered complete NVU.	Designed to replicate complex cell–cell interactions and pathophysiological responses	High	Research on complex brain diseases and exploration of individualized treatment

BBB: blood-brain barrier; TEER: transendothelial electrical resistance; 3D: three dimensional; NVU: neurovascular unit.

2.2 Techniques for evaluating the permeability of *in vitro* BBB models

In studies of *in vitro* BBB models, it is necessary to precisely assess the barrier's permeability. Currently, the determination of P_{app} (Di et al., 2013) and the measurement of TEER (Srinivasan and Kolli, 2018; Tu et al., 2020; Vigh et al., 2021; Yin et al., 2022; Nazari et al., 2023; Malik et al., 2025; Srinivasan and Kolli, 2025) are the two most extensively utilized and widely accepted methods for the functional validation of *in vitro* BBB models (Fig. 4).

2.2.1 P_{app} determination of *in vitro* BBB models

The principle of P_{app} determination involves quantitatively measuring the transport rate of a specific substance across a cellular monolayer under controlled laboratory conditions to assess barrier functionality. Its advantages include operational simplicity, low cost, and ease of implementation for high-throughput screening. Furthermore, it allows the simultaneous use of tracer molecules of varying molecular weights to evaluate the BBB's selectivity for molecules of different sizes. For instance, Ito et al. established a highly functional *in vitro* BBB model by co-culturing human BMECs with astrocytes and pericytes in a Transwell system (Ito et al., 2019). Using unidirectional transport assays, they determined P_{app} values for a series of compounds, revealing that those for highly permeable drugs were substantially higher than those for low-permeability markers, spanning a 287-fold dynamic range. Compared to monoculture models, the triple-culture model exhibited a tighter barrier and significantly enhanced functionality of efflux transporters such as P-gp. This model provides a reliable tool for assessing the brain penetration potential of compounds in CNS drug discovery. In a separate study, Metzger et al. systematically determined P_{app} values to functionally characterize the barrier properties of a stem cell-derived BBB model (Appelt-Menzel et al., 2017). By employing hydrophilic markers of different molecular weights to assess paracellular permeability, the model demonstrated a characteristic molecular-weight-dependent permeation profile: P_{app} values decreased markedly from approximately 1.5 μm/min for small molecules to 0.0030 μm/min for 40 kDa dextran. Furthermore, transcellular permeability and active transport function were evaluated using a panel of reference drugs, with data normalized against diazepam. The quadruple-culture model was found to have the tightest barrier, exhibiting significantly lower permeability for large molecules than monoculture models. Additionally, treatment with the P-gp inhibitor verapamil resulted in a significant increase in the P_{app} value of its substrate, rhodamine 123, confirming the presence and correct polarization of functional efflux transporters within the model. These systematic P_{app} determinations demonstrate that the quadruple-co-culture BBB model exhibits excellent barrier integrity and holds significant potential for predicting drug permeability.

2.2.2 TEER measurement of *in vitro* BBB models

TEER measurement is a critical method for assessing the integrity and permeability of cellular monolayers (Deli et al., 2005; Benson et al., 2013). This technique operates on the principle of quantifying electrical resistance across a cell layer, offering distinct advantages such as high sensitivity and real-time monitoring. It can detect early-stage, subtle alterations in barrier function induced by pharmaceuticals, cytokines, or pathological conditions. Furthermore, TEER enables longitudinal, dynamic tracking of barrier functionality within the same set of samples across processes such as drug screening or disease modeling. It directly reflects the barrier's physiological functional state rather than merely reporting protein expression levels. TEER measurement techniques are broadly categorized into two approaches: the Ohm's Law method and impedance spectroscopy (Srinivasan et al., 2015). The Ohm's Law method involves applying an alternating current across electrodes on either side of the cell layer, measuring the resulting resistance, and multiplying it by the membrane surface area to obtain the TEER value. This value is normalized to a blank control. A higher measured resistance corresponds to a greater TEER value, indicating a more intact barrier. While the primary advantage of the Ohm's Law method is its operational simplicity, its measurements are susceptible to influences from electrode

positioning and current density uniformity. Conversely, impedance spectroscopy is performed by applying a small-amplitude alternating current excitation signal with frequency sweeps and measuring the resulting current's amplitude and phase response. By acquiring more comprehensive electrical characteristics of the cell layer using frequency scanning and fitting the data to equivalent circuit models, this approach provides a more accurate determination of the TEER value (Douville et al., 2010).

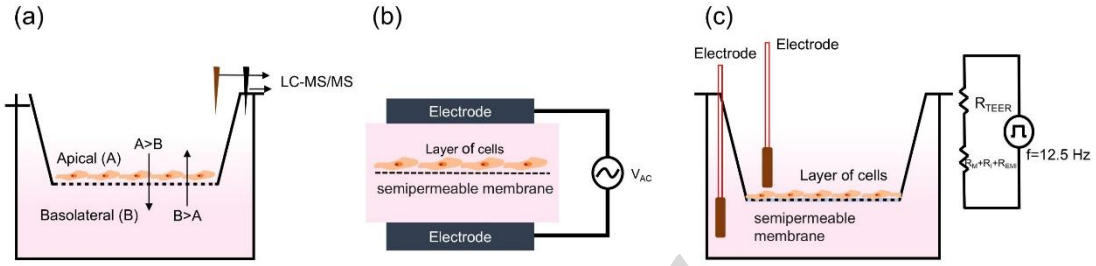

Fig. 4 The permeability assessment of the *in vitro* BBB model. (a) Measurement of the apparent permeability coefficient (P_{app}). (b) Measurement of TEER using impedance spectroscopy. (c) Measurement of TEER using Ohm's Law. The total electrical resistance includes the ohmic resistance of the cell layer R_{TEER}, the cell culture medium R_M, the semipermeable membrane insert R_I, and the electrode medium interface R_{EMI}.

TEER measurement technology is rapidly advancing toward standardization, integration, and high-throughput capabilities. For example, Van Der Helm et al. developed a four-electrode TEER system for direct quantification in organ-on-a-chip platforms. This technique employs six distinct electrode configurations for measurements and uses a derived formula to directly calculate the resistance of the cellular barrier and the membrane, effectively eliminating background noise from microchannel resistance (Van Der Helm et al., 2016). This method achieved stable, reliable TEER measurements (22 Ω·cm²) in a hCMEC/D3 cell-based BBB-on-a-chip model, with results consistent with those produced by traditional Transwell systems. Furthermore, this approach does not interfere with microscopic observation of the cell layer, significantly enhancing the reliability of quantitative barrier function assessment on organ-on-a-chip platforms. Separately, Badiola-Mateos et al. introduced a novel multi-frequency TEER sensor array for real-time monitoring of BBB integrity (Badiola-Mateos et al., 2021). This technology integrates a microfluidic chip with embedded gold electrodes and couples it with broadband impedance spectroscopy, acquiring impedance data across a frequency range of 100 Hz to 10 MHz. By incorporating a machine learning algorithm, the system enables high-precision identification and classification of different physiological stages, including barrier formation, maturation, injury, and recovery. This system not only possesses multi-position, non-invasive dynamic monitoring capabilities, but also yields measurement results that show a strong correlation with changes in tight junction proteins as revealed by immunofluorescence staining. This technology provides a more powerful and reliable *in vitro* evaluation tool for drug delivery research and the analysis of barrier-related pathological mechanisms.

3 Imaging techniques for BBB permeability assessment

In vitro models of the BBB partially recapitulate its structure and function, and corresponding permeability assessment techniques are indispensable for research on CNS diseases and for early-stage screening of related therapeutics. However, if subtle regional changes in BBB integrity need to be detected, multiple *in vivo* imaging techniques are required, such as computed tomography (CT), magnetic resonance imaging (MRI), positron emission tomography (PET), and optical imaging (Table 2). These methods can dynamically monitor changes in

BBB permeability, molecular transport processes, and intercellular interactions, providing direct visual evidence for understanding the pathological mechanisms of CNS disorders and for evaluating therapeutic efficacy.

3.1 Magnetic resonance imaging

3.1.1 Non-contrast MRI

Water molecules freely traverse the BBB and exhibit high sensitivity to early changes in the BBB under pathological conditions (Cornford and Hyman, 1999). As the main source of MRI signals, water molecules can provide sufficient sensitivity without exogenous contrast agents, making them an ideal endogenous tracer for assessing BBB function. Arterial spin labeling (ASL), as a representative technique, has been widely employed for the quantitative evaluation of cerebral perfusion and other hemodynamic parameters through the manipulation and modeling of the water signal in blood (St. Lawrence et al., 2000; Zhou et al., 2001; Parkes and Tofts, 2002; Fernández-Seara et al., 2005; Wang et al., 2007; Liu et al., 2011; St. Lawrence et al., 2012). Based on the ASL principle, Lin et al. developed a non-contrast MRI technique that quantifies the water-extraction fraction and permeability parameters by detecting the signal from venous blood flowing into the superior sagittal sinus, thereby enabling the quantitative assessment of BBB water permeability (Lin et al., 2018). The sensitivity of this technique is significantly enhanced when data are acquired under mild hypercapnic conditions, opening a new avenue for the non-invasive, safe monitoring of BBB function.

In recent years, this technique has demonstrated potential for application in various neurological disease models. Mouchtouris et al. explored the use of non-contrast MRI to assess BBB permeability in patients with acute ischemic stroke (Mouchtouris et al., 2024). They employed a DP-pCASL sequence to measure the water exchange rate and combined it with NODDI sequence analysis to characterize tissue microstructure. The results revealed that the water exchange rate was significantly correlated with both the time post-stroke and tissue parameters, and was also influenced by mechanical thrombectomy. Xiong et al.'s research on AD used the non-contrast MRI technique to conduct a longitudinal study in an AD mouse model. They found that as the disease progressed, both BBB water permeability and transmembrane water exchange in the hippocampal region were significantly increased, accompanied by abnormal polarization of the AQP4 water channel protein (Xiong et al., 2025). These impairments in key components of the glymphatic system are significantly associated with the deposition of Aβ and tau proteins, revealing the critical role of compromised waste clearance in the pathogenesis of AD.

3.1.2 Dynamic contrast-enhanced magnetic resonance imaging

Dynamic contrast-enhanced MRI (DCE-MRI) is another MRI method that requires intravenous injection of gadolinium-based contrast agents. Through repeated scanning, it captures signal changes caused by trans-BBB extravasation of contrast agents and quantifies the leakage rate of contrast agents from the bloodstream into brain tissue, thereby assessing the degree of BBB opening. Over the past two decades, DCE-MRI has undergone substantial development as a technique for evaluating BBB leakage *in vivo* (Heye et al., 2014; Raja et al., 2018).

DCE-MRI has been used to study cerebral small vessel disease (cSVD). Zhang et al. used a dual-temporal-resolution DCE-MRI protocol combined with the Patlak pharmacokinetic model, which allowed not only the quantification of BBB leakage rate but also an innovative assessment of leakage volume (Zhang et al., 2019). Their results indicated that within white matter hyperintensity (WMH) regions of cSVD patients, the spatial extent of leakage was expanded, yet the leakage rate was reduced, suggesting a chronic, diffuse leakage process. In contrast, during healthy aging, the leakage rate was correlated with cognitive decline. Further elucidating this, Verstappen et al. utilized high-resolution DCE-MRI to reveal that BBB impairment in cSVD patients exhibits spatial heterogeneity: leakage was more pronounced in the normal-appearing white matter (NAWM) distal to WMH borders, forming a proximal-to-distal gradient pattern (Verstappen et al., 2025). This

indicates that BBB damage in cSVD is not uniformly distributed but is closely associated with microvascular architecture and local blood flow regulation. These findings provide crucial imaging evidence for understanding the spatial heterogeneity of BBB impairment across populations and underscore the potential of using BBB leakage as a significant biomarker for early diagnosis and therapeutic evaluation of cSVD.

DCE-MRI has provided pivotal evidence that elucidates BBB dysfunction in the early stages of AD. Van De Haar et al. conducted a pioneering study showing no significant difference in leakage rate across global NAWM and cortical gray matter (GA) in early AD patients (Van De Haar et al., 2016). This suggests that BBB dysfunction in early AD primarily manifests as a diffuse, widespread pattern of subtle leakage, rather than a marked increase in the local leakage rate. This study provided the first *in vivo* confirmation in the human brain that widespread BBB disruption is a principal pathological feature of early AD, offering crucial imaging evidence for understanding the role of NVU in AD pathogenesis. Nation et al. further investigated the relationship between BBB disruption and early cognitive impairment through a combined analysis of DCE-MRI and cerebrospinal fluid (CSF) biomarkers (Nation et al., 2019). Their results demonstrated that during the early stages of cognitive decline, the BBB exhibits significant leakage within the hippocampus and its subfields. Importantly, this disruption was found to be independent of changes in canonical AD biomarkers, namely Aβ and tau pathology. Concurrently, elevated levels of soluble platelet-derived growth factor receptor β (sPDGFRβ) in the CSF also suggested an association between BBB disruption and injury to cerebral capillary pericytes. This study provided the first human evidence identifying BBB disruption as an independent biomarker for early cognitive impairment, highlighting the independent role of NVU dysfunction in the pathogenesis of AD and suggesting a new direction for early diagnosis and intervention.

Furthermore, DCE-MRI has been applied to psychiatric disorders. Shang et al. provided the first *in vivo* evidence of significantly elevated BBB permeability in emotion-related brain regions—including the olfactory cortex, caudate nucleus, and thalamus—in patients with major depressive disorder (MDD) (Shang et al., 2024). Importantly, this increase in permeability was positively correlated with the severity of depressive symptoms, providing direct imaging evidence for the involvement of BBB disruption in the pathophysiology of MDD.

In summary, DCE-MRI has matured into an indispensable tool for quantifying BBB permeability *in vivo*. The foremost challenge remains standardizing acquisition and analytical pipelines to enable robust multicenter comparisons. Key frontiers include defining the prognostic value of distinct leakage phenotypes and validating BBB permeability metrics as endpoints for interventional trials. Looking ahead, the translational potential of DCE-MRI is substantial. Its unique capacity to quantitatively track neurovascular health *in vivo* positions it as a crucial tool for guiding precision medicine approaches, validating BBB integrity as a therapeutic target, and serving as a biomarker in early-phase clinical trials.

3.2 Computed tomography

Computed tomography (CT) imaging produces cross-sectional images based on the differential X-ray absorption by various tissues. In BBB permeability assessment, CT primarily relies on the distribution of iodinated contrast agents in brain tissue: an intact BBB prevents contrast agent extravasation, whereas BBB disruption allows leakage into the interstitial space, resulting in localized hyperdensity on CT images, termed "contrast enhancement." Although CT offers advantages such as rapid scanning, widespread availability, and high sensitivity for detecting hemorrhage and calcification—making it suitable for initial screening in acute brain injury—its application in BBB research is limited by insufficient quantitative capability, low soft-tissue contrast, radiation exposure, and limited functional information (Pardridge, 2005). The advent of CT perfusion (CTP) imaging represents a major advance for CT in BBB research. This technique involves the rapid intravenous bolus administration of a contrast agent, followed by continuous dynamic scanning of a selected tissue plane to generate time–density curves. BBB permeability parameters are then calculated by applying pharmacokinetic models (Miles and Griffiths, 2003). For instance, Xu et al. used CTP to demonstrate a

significant increase in BBB permeability in the perihematomal region within 24–72 h following acute spontaneous basal ganglia hemorrhage, which correlated positively with both hematoma and perihematomal edema volumes. This revealed that BBB disruption is a critical factor in edema formation (Xu et al., 2017). Furthermore, Chen et al. found that relative permeability parameters derived from CTP in hypoperfused regions could effectively predict the risk of parenchymal hematoma after mechanical thrombectomy in ischemic stroke patients, offering superior predictive value compared to conventional imaging markers (Chen et al., 2024b).

Spectral CT, another significant technological advancement, is based on the principle that different materials exhibit distinct X-ray attenuation characteristics at different energy levels. Performing scans with two different X-ray energy spectra simultaneously or in rapid succession enables material decomposition (Johnson et al., 2007; Siegel et al., 2016; Winklhofer et al., 2017). Spectral CT can generate iodine density maps and virtual non-contrast images, thereby enhancing the detection of subtle BBB leakage while reducing artifacts and contrast agent dosage (Grkovski et al., 2023a). Research by Grkovski et al. demonstrated that this technique allows for clearer differentiation between ischemic tissue and normal brain parenchyma post-stroke, enabling more precise lesion characterization and quantitative assessment (Grkovski et al., 2023b). Consequently, spectral CT provides a powerful imaging tool for the more accurate evaluation of BBB injury in stroke, with the potential to optimize clinical management and prognostic evaluation.

3.3 Positron emission tomography

Positron emission tomography (PET), as a highly sensitive molecular imaging technique, enables *in vivo*, non-invasive assessment of BBB permeability by tracking the distribution and kinetic processes of specific radiolabeled tracers. It is indispensable for both basic research and clinical exploration (Salehi Farid et al., 2025). PET is the most sensitive imaging modality, capable of detecting ligand concentrations in the picomolar to femtomolar levels. A major strength of PET lies in its capacity, through dynamic PET scanning and compartmental modeling, to precisely calculate quantitative parameters such as the tracer uptake rate or permeability–surface area product at the BBB. This transcends simple qualitative assessments of "present or absent," enabling precise comparisons across individuals and time points, thereby providing objective metrics for monitoring disease progression or therapeutic response. Additionally, PET offers targeting specificity; by selecting different radiotracers, it can specifically investigate various BBB functions. PET imaging has significantly deepened our understanding of BBB dysfunction across a variety of conditions and has been widely used in neurodegenerative diseases (Mensch et al., 2009), epilepsy (Löscher and Friedman, 2020) and brain tumor imaging. Furthermore, PET is used in drug development and therapeutic evaluation, demonstrating considerable translational potential to guide rational drug use and develop novel therapeutic strategies.

The application of PET imaging technology in BBB permeability research is continuously expanding, revealing significant scientific value and clinical potential. For example, Chen et al. developed a radiotracer ([^{18}F] FAI-NEB) that rapidly binds to serum albumin and used dynamic PET to assess tumor vascular leakage (Chen et al., 2017). They proposed a simplified quantitative parameter (Ps) that quantifies vascular leakage by analyzing the difference in slope between the tumor and blood time–activity curves. This method demonstrated high consistency with traditional Evans Blue (EB) extraction and DCE-MRI results, thereby providing a new tool for ultra-early treatment evaluation. In another study, Chung et al. used a non-invasive method that combined high temporal-resolution total-body PET imaging with kinetic modeling to quantitatively measure the permeability–surface area product (PS) of molecules at the BBB (Chung et al., 2025). Using multiple tracers (e.g., ^{18}F-FDG, ^{18}F-fluciclovine, and ^{11}C-butanol), they simultaneously estimated cerebral blood flow and the BBB transport rate constant K_1 in a single scan, from which the molecular PS was calculated. In studies of healthy aging and patients with metabolic dysfunction-associated steatohepatitis (MASH), they found that BBB permeability to FDG decreases with advancing age, providing a novel tool for *in vivo* investigation of molecular BBB permeability and research into brain–body interactions.

In brain disease imaging, multimodal imaging detection of BBB permeability can be achieved by

designing multifunctional probes. Dai et al. designed a novel fluorescent probe based on a quinoline-malononitrile (QM) scaffold, which has the capabilities of near-infrared fluorescence (NIRF), MRI, and PET trimodal imaging (Dai et al., 2025). This probe can efficiently cross the BBB and specifically bind to cerebral Aβ plaques, enabling high-sensitivity, quantitative PET-CT imaging. Significant radioactive accumulation (1.7 %ID/g) was observed in the brains of AD model mice only 2 minutes post-injection, which was markedly higher than that in wild-type mice (0.9 %ID/g). Simultaneously, the brain's metabolic process could be dynamically monitored. Its favorable brain penetration and biosafety were also validated in a beagle dog model. This work integrated NIRF, MRI, and PET imaging capabilities into a single molecular probe, with PET providing key quantitative indicators, representing a powerful multifunctional imaging tool for the early diagnosis, pathological research, and drug screening of AD.

PET imaging is also used to evaluate the methods for regulating the BBB in AD models. Li and colleagues have explored the application of focused ultrasound (FUS) to induce transient, reversible BBB opening. This innovative approach enhances the cerebral delivery of the radiotracer [^{68}Ga] STZL4110 in AD model mice, thereby improving the signal-to-noise ratio of PET imaging. These findings contribute to the development of novel strategies for optimizing brain-targeted drug delivery and pathological imaging (Li et al., 2025b). Furthermore, Toyohara has elucidated the fundamental principles and significance of PET imaging for investigating P-gp function at the BBB (Toyohara, 2016). As a critical efflux transporter, P-gp directly modulates the permeation of pharmaceuticals and toxins into the CNS, thereby influencing therapeutic efficacy and toxicological profiles in CNS disorders (Juliano and Ling, 1976; Ambudkar et al., 1999). The development and application of PET tracers such as [^{11}C] verapamil enable non-invasive *in vivo* assessment of changes in functional BBB permeability. P-gp hyperfunction may contribute to multidrug resistance, while hypofunction potentially elevates neurotoxicity risks. These advancements highlight the utility of P-gp PET imaging for mechanistic investigations and clinical pharmacokinetic guidance for conditions such as epilepsy (Feldmann et al., 2013; Bauer et al., 2014) and depression (De Klerk et al., 2009).

In summary, PET is evolving from a descriptive research tool into a quantitative platform for precision neurovascular medicine. Standardizing tracer protocols and simplifying complex kinetic models for clinical adaptation will provide robust support for the early diagnosis of neurological disorders, drug delivery, and efficacy assessment.

Table 2 *In vivo* imaging technology for BBB assessment

Imaging technology		Application in BBB assessment	Sensitivity	Resolution	Penetration Depth
MRI	NC-MRI	Assessment of the BBB integrity through water MRI signals	Relatively low (based on water proton signal)	10–100 μm	/
	DCE-MRI	Evaluation of BBB leakage based on contrast agent (gadolinium) injection	Medium (dependent on contrast agent)	1–2 mm	/
CT	Conventional CT	Evaluation of the BBB permeability based on X-Ray signal of contrast agents(iodine)	Relatively low (10^{-6} mol/L)	50 μm	/
	CTP	Quantitative assessment of BBB damage by analyzing the time–density curve of contrast agent.	Moderate (dependent on iodine concentration)	0.5–1 mm	Equivalent to CT (limited by detector coverage)
	Spectral CT	Precise analysis of BBB leakage of contrast agent based on X-ray energy spectrum	Specific substances (iodine) is higher than that of conventional CT	50–200 μm	/
PET		Dynamic quantitative analysis of the BBB permeability of radionuclide-labeled substances（drug, protein, peptide）	High (10^{-11}–10^{-12} mol/L)	1–2 mm	/
FI	NIR-II	Real-time, dynamic visualization of the entire process of BBB bade on NIR-II fluorescence imaging	High (10^{-9}–10^{-12} mol/L)	2–3 mm (deep dependency)	3 cm
	TPM	High-resolution assessment of molecular crossing of the BBB based on *in vivo* or cellular-level FI	High	Submicron scale (~0.65 μm)	1 mm
PAI		A comprehensive assessment of BBB permeability by combining high-resolution vascular structure and function information obtained from fluorescence and ultrasound imaging	High	0.4 mm–0.6 mm	~1 cm

MRI: magnetic resonance imaging; CT: computed tomography; PET: positron emission tomography; FI: fluorescence imaging; PAI: photoacoustic imaging; NC-MRI: non-contrast MRI; DCE-MRI: dynamic contrast-enhanced MRI; CTP: CT perfusion; NIR-II: near-infrared II; TPM: two-photon microscopy.

3.4 Fluorescence imaging

Fluorescence imaging (FI), with its non-invasive nature, high sensitivity, superior spatiotemporal resolution, and real-time dynamic imaging capabilities, has become a pivotal tool in biomedical research. It is widely used for multidimensional visualization at the molecular, cellular, tissue, and even *in vivo* levels. Particularly in preclinical investigations of microscopic mechanisms, such as BBB permeability, this technique offers rapid, intuitive dynamic monitoring, demonstrating irreplaceable advantages (Hong et al., 2017). The development of super-resolution optical imaging instruments, *in vivo* imaging equipment, and imaging probes has further broadened the scope of fluorescence imaging. It can be used for dynamic BBB detection in living organisms and for high-resolution imaging of *in vitro* BBB models or excised tissues.

3.4.1 *Ex vivo* brain tissue BBB fluorescence imaging

Ex vivo fluorescence imaging is a well-established method for evaluating BBB permeability. This technique typically involves intravenous administration of fluorescent tracers such as FITC-dextran or EB, followed by transcranial perfusion, brain extraction, and cryosection preparation following the experimental procedure. The spatial distribution and fluorescence intensity of these tracers are then examined using confocal or fluorescence microscopy to obtain two-dimensional information on BBB leakage. This approach clearly visualizes whether the tracer remains confined within the blood vessels or has extravasated into the perivascular parenchyma, enabling precise anatomical localization of leakage sites. Zhang et al. systematically evaluated electroacupuncture stimulation at specific frequencies (2/100 Hz) for its effect on rat BBB permeability using EB and 20 kDa FITC-dextran combined with confocal microscopy (Zhang et al., 2020). Results demonstrated that electroacupuncture significantly enhanced BBB permeability; this enhancement was reversibly restored within 12 h post-stimulation. Imaging revealed tracer extravasation in the cerebral cortex and perivascular regions, indicating that electroacupuncture induces reversible BBB opening by modulating tight junction proteins (e.g., ZO-1, occludin) and promoting endothelial gap formation.

Shumer-Elbaz et al. developed a non-invasive BBB opening technique using low-frequency FUS combined with microbubbles to deliver ionizable lipid nanoparticles (LNP) to glioblastoma regions. They assessed BBB opening by examining EB and fluorescent dextran extravasation in brain sections, and used Cy5-labeled siRNA-LNP fluorescence to confirm translocation and tumor accumulation (Elbaz et al., 2025). Confocal microscopy revealed the distribution of Cy5-siRNA-LNP within tumor tissue, with co-localization in GFP-labeled tumor cells indicating cellular uptake. DAPI staining further illustrated the distribution of LNP among non-tumor cells in the tumor microenvironment. This strategy overcomes the limitations of the BBB for LNP delivery, enabling LNP-based therapies for neurological disorders. While ex vivo imaging provides intuitive spatial localization and semi-quantitative data, dynamic monitoring of BBB permeability in living animals requires *in vivo* imaging technologies.

3.4.2 *In vivo* fluorescence imaging techniques

In vivo fluorescence imaging techniques include wide-field, near-infrared I/II (NIR-I/II), and multiphoton fluorescence imaging. Conventional wide-field fluorescence imaging is limited by its low throughput and invasiveness. Early implementations required cranial window implantation or skull thinning for cerebral optical imaging (Yang et al., 2010; Wang et al., 2019), although the method remains advantageous due to its technical simplicity, cost-effectiveness, compatibility with diverse fluorescent probes, and suitability for large-scale screening and longitudinal studies. However, it offers limited spatial resolution and poor penetration into deep brain structures, and yields semi-quantitative results that are susceptible to multiple confounding factors. With advances in microscopy, NIR-I/II fluorescence imaging has gained widespread adoption. Biological tissues exhibit significantly reduced absorption and scattering of near-infrared light, allowing greater penetration depth, improved signal-to-noise ratio, and enhanced spatial resolution.

Compared to conventional visible-light or NIR-I imaging (1–2 cm depth), NIR-II (1000–1700 nm) achieves substantially greater penetration depth (3 cm) along with superior signal-to-noise ratio and spatial resolution due to minimized photon scattering and absorption in tissue (Hong et al., 2012; Cao et al., 2020). Recent years have seen notable advances in novel NIR-II probes. Wang et al. systematically modified aniline groups in dye molecules to create a series of NIR-II fluorophores with emission wavelengths ranging from 800 to 1400 nm (Wang et al., 2022). These dyes exhibit high extinction coefficients, large Stokes shifts, excellent brightness, and superior photostability and biostability compared to the clinical dye indocyanine green (ICG). Notably, certain dyes (e.g., BF_1 and BF_6) with molecular weights below 450 Da and optimal lipophilicity efficiently cross the intact BBB, which enables non-invasive, high-fidelity NIR-II fluorescence imaging of the mouse brain parenchyma. Functional probes have further expanded the applications of NIR-II imaging. Lu et al. developed a novel NIR-II imaging probe, DGC, that targets connective tissue growth factor (CTGF) for early AD detection prior to Aβ plaque formation (Lu et al., 2024). Comprising gold nanoclusters and cyclic peptides, DGC exhibits high BBB affinity (KD=21.9 nM) and penetration ability, allowing clear visualization of elevated cerebral CTGF levels in 1-month-old APP/PS1 transgenic mice. Additionally, this probe supports multimodal analysis, including fluorescence imaging, chromogenic reaction, and ICP-MS quantification, and has been validated in human AD brain sections. Notably, Zhang et al.'s pioneering research achieved the first real-time multiplexed NIR-II imaging technology in live mammals enhanced by deep learning, a breakthrough that marks a crucial step toward the clinical translation of biomedical optical imaging technologies (Zhang et al., 2023). However, the practical application of this technology in assessing BBB permeability still faces several translational hurdles. These include reduced signal fidelity due to increased imaging depth, the lack of clinically validated BBB-specific tracers, and challenges related to the *in vivo* stability, biosafety, and scalable production of NIR-II imaging probes.

The multiphoton microscope (MPM) is an advanced nonlinear optical imaging technology that enables rapid, label-free imaging of biological tissues at subcellular resolution with minimal photodamage (Li et al., 2014; Chen et al., 2025; Qiu et al., 2025). Two-photon microscopy (TPM), the most widely used form of MPM, employs near-infrared femtosecond laser pulses to excite fluorescence through the simultaneous absorption of two low-energy photons. This approach increases imaging depth (up to hundreds of micrometers) while reducing phototoxicity and photobleaching, making it the standard for real-time, *in vivo* observation of cerebral microstructures (Denk et al., 1990). In BBB research, TPM allows dynamic, real-time monitoring of leakage processes. Following intravenous injection of fluorescent tracers (e.g., FITC-dextran), the technique can capture the complete spatiotemporal dynamics of tracer extravasation from cerebral vessels, enabling precise localization of leakage sites. For example, Lee et al. used real-time *in vivo* two-photon imaging to study the effects of chronic restraint stress on the mouse cerebrovascular system (Lee et al., 2018). Their research revealed that chronic stress induced generalized vasoconstriction, reduced total cerebrovascular volume, and concomitant BBB hyperpermeability. These pathological changes were associated with upregulated cerebral VEGF-A expression and downregulated tight junction protein Claudin-5.

Furthermore, TPM serves as a critical tool for evaluating the impact of pharmacological or physical interventions (e.g., FUS) on BBB permeability, enabling real-time discrimination between reversible opening and irreversible structural damage. Poon et al. investigated the effects of FUS combined with microbubbles on Aβ plaques in AD model mice (Poon et al., 2018). Using *in vivo* real-time two-photon imaging, they visualized immediate BBB opening post-FUS (evidenced by dextran leakage) and tracked individual Aβ plaques over time. Results indicated that a single FUS session simultaneously enhanced BBB permeability and reduced plaque volume by 62% within two days, with effects persisting for two weeks. This suggests that FUS may facilitate Aβ clearance through endogenous mechanisms (e.g., immune cell infiltration) by inducing temporary, controllable BBB opening. Subsequent MRI-guided repeated FUS treatments confirmed the feasibility and cumulative efficacy of this protocol. This groundbreaking work established the direct causal relationship and temporal sequence between FUS-induced BBB opening and Aβ clearance at the *in vivo* level, providing crucial imaging

evidence for developing FUS as a non-invasive, repeatable therapeutic strategy for AD.

Although TPM offers unparalleled advantages in preclinical studies, its extremely shallow penetration depth and requirement for craniotomy or the implantation of a transparent window limit its clinical translation potential. Consequently, TPM is primarily used for basic research.

3.5 Photoacoustic imaging

Photoacoustic imaging (PAI) is an emerging non-invasive biomedical imaging modality that combines the high contrast specificity of optical imaging with the penetration depth of ultrasonic imaging. Its principle relies on the generation of ultrasonic waves via thermoelastic expansion following light absorption in biological tissues, in which the amplitude of the emitted ultrasound signal reflects local optical properties (Hui et al., 2016; Chen et al., 2024a; Wang et al., 2024). By exploiting the distinct absorption profiles of biomolecules and using multiwavelength imaging, PAI enables high-contrast visualization of multiple molecular targets. This capability enables it to overcome the depth limitations of conventional optical imaging, achieving several centimeter penetration while preserving high spatial resolution, making it particularly suitable for imaging deep brain structures (Liu et al., 2021; Lin and Wang, 2022; Zhu et al., 2024).

The potential of PAI for assessing BBB integrity has been vividly demonstrated by recent studies utilizing novel molecular probes. Qin et al. (2025) developed a novel fluorescence/photoacoustic probe (namely, IVTPO) based on an electron donor-π-acceptor (D-π-A) system for glioblastoma (GBM) imaging. This probe exhibits near-infrared absorption (572 nm), high molar extinction coefficient (12.29×10^4 M^{-1} cm^{-1}), excellent photostability, and BBB penetration capability. In GBM mouse models, intravenous administration of IVTPO enabled high-resolution, real-time, non-invasive PAI through the intact skull, clearly delineating tumor location, abnormal vascular structures, and early probe extravasation in peritumoral regions. Compared to the commercial dye EB, IVTPO showed superior sensitivity and targeting, detecting subtle leakage before full BBB disruption, thereby offering a powerful tool for early GBM diagnosis. PAI has also shown considerable promise in the diagnosis of neurodegenerative diseases. Li et al. reported a D-π-A molecular probe, DMA-Te, engineered through thiopyridine modulation for high-contrast PAI of Aβ plaques in AD (Li et al., 2025a). By incorporating a Te atom as an electron acceptor, this probe achieves a significantly red-shifted absorption peak at 794 nm in the near-infrared region while maintaining a low fluorescence quantum yield (0.0006), thereby favoring strong photoacoustic signal generation. Upon binding to Aβ fibrils, DMA-Te maintained a twisted intramolecular charge-transfer state and efficient non-radiative decay, preserving excellent photoacoustic performance. Furthermore, the probe exhibits favorable BBB penetration (20.8% penetration rate) and high Aβ-binding affinity. In AD mice, a dual-wavelength PAI system successfully accomplished simultaneous, high-resolution imaging of both Aβ plaques and cerebral vasculature, highlighting its potential for early diagnosis. The integration of PAI technology with specific molecular probes provides a powerful tool for early diagnosis and pathological investigation of neurological disorders, particularly offering unique advantages for high-resolution, deep-penetration imaging.

Despite promising preclinical advances, the clinical translation of PAI faces dual challenges. First, the development of molecular probes is constrained by challenges in biocompatibility, pharmacokinetics, and scalable production. Probes such as IVTPO and DMA-Te, for instance, require extensive safety validation beyond rodent models. Second, the field lacks standardized quantitative methods, currently relying on descriptors such as ‘signal enhancement’ rather than offering universally comparable, dynamic metrics of BBB permeability. To advance its application, future efforts should focus on developing novel probes, establishing robust quantitative standards, and validating reliability through multicenter clinical studies.

4 Artificial intelligence in enhancing BBB permeability assessment

In vitro BBB models and *in vivo* imaging techniques remain indispensable tools for assessing BBB

permeability. However, these methods face challenges, including time-consuming procedures, high costs, and limited mechanistic insights, rendering them inadequate for modern drug development. In this context, the deep integration of artificial intelligence (AI) is reshaping the research paradigm. By efficiently integrating multi-omics data, dynamically simulating molecule–barrier interactions, intelligently optimizing drug design workflows, and enabling precise quantitative analysis of biomedical imaging information, AI is emerging as a critical tool for overcoming bottlenecks in CNS drug development (Clark, 2003; Saxena et al., 2019).

Currently, key AI approaches for predicting BBB permeability (Grant et al., 2025) include classical machine learning based on chemical descriptors (Yuan et al., 2018; Shaker et al., 2021; Shaker et al., 2023), deep learning utilizing graph neural networks (Withnall et al., 2020; Jiang et al., 2021; Dey and Ning, 2024), and natural language processing based on simplified molecular input line entry system (SMILES) sequences (Tevosyan et al., 2022; Wen et al., 2022; Rollins et al., 2024). These models significantly accelerate drug development by predicting candidate permeability and elucidating BBB interactions. In particular, descriptor-based models offer a key advantage in their interpretability, providing mechanistic insights into prediction outcomes. For instance, Liu et al. employed support vector machine (SVM), random forest (RF), and extreme gradient boosting (XGBoost) algorithms with 1,757 compounds and nine molecular fingerprints to construct an ensemble of 27 base classifiers, optimizing BBB permeability predictions (Liu et al., 2021). Their study calculated the average reduction in the Gini coefficient for molecular fingerprints using a random forest model, enabling clear quantification of the contributions of different molecular substructures to prediction outcomes. It explicitly identified a strong correlation between oxygen-containing polar groups (e.g., carboxylic acids, polyhydroxy structures) and BBB impermeability. However, such models rely on predefined molecular descriptors, which may fail to capture the complex interactions influencing BBB permeability. In contrast, deep learning with graph neural networks demonstrates significant potential by directly representing molecular structure and spatial information. For example, Group Graph, as a novel substructure-level molecular representation method, is applicable for predicting molecular properties and optimizing structures in drug discovery (Cao et al., 2024). One key advantage of Group Graph is its balance between computational efficiency and representational capacity, achieved by simplifying graph structures while maximally preserving chemical information. However, this process simplifies stereochemical information and completely omits three-dimensional structural details, potentially causing model failure in critical scenarios and limiting its application in high-value contexts. Language-based BBB permeability prediction methods treat SMILES strings as textual input, using encoders to extract chemically meaningful embeddings without relying on predefined descriptors. Their advantage lies in enabling end-to-end learning without predefined features, making them suitable for large-scale pretraining and transfer learning. However, their performance typically falls short of that of traditional classical and graph models, with limitations including poor interpretability and strong reliance on textual representations. One noteworthy study proposes MolPMoFiT, a transfer learning approach for molecular property prediction (Li and Fourches, 2020). After self-supervised pretraining on millions of compounds, it can be fine-tuned on small datasets, directly processing SMILES strings without manual feature engineering. Experiments show it matches or surpasses state-of-the-art models on tasks such as BBB permeability and is particularly adept at improving predictive performance in data-sparse drug discovery scenarios.

AI also plays a crucial role in precisely quantifying and dynamically monitoring BBB permeability by automating the analysis of complex biomedical images. Jackson et al. developed a novel computational approach to optimizing CNSPET tracer design and enhancing its translational success rate (Jackson et al., 2021). The team constructed a dataset comprising 140 successful and unsuccessful PET tracers. By analyzing seven key physicochemical properties—including clogP and tPSA—they identified significant differences between successful and non-penetrating tracers in tPSA and clogP. Based on these findings, the team developed a computational screening tool demonstrating exceptional specificity (96.7%) and positive predictive value (97.4%) in distinguishing successful from non-penetrating tracers. This tool enables early elimination of likely

failures, thereby conserving preclinical resources. This work provides valuable data and efficient computational tools to support the rational design of future CNS PET tracers. In a different application, Zhang et al. developed a novel method combining optical coherence tomography (OCT) with deep learning (pix2pix cGAN) for rapid, non-invasive visualization and quantification of microvessels in three-dimensional BBB models (Zhang et al., 2023). By outperforming traditional morphological processing and random forest methods, this deep learning approach achieves superior accuracy in segmenting vessels in low-contrast OCT images. It thus provides an efficient, label-free analytical tool for assessing permeability in BBB models and for drug screening applications.

5 Conclusion and future directions

In conclusion, precise assessment of BBB permeability is essential for elucidating mechanisms of neurological disease and advancing drug development. *In vitro* models serve as crucial screening platforms during early drug discovery, having evolved from traditional static Transwell systems to dynamic models incorporating fluid shear stress (e.g., hollow fiber reactors and microfluidic chips) and, more recently, to highly biomimetic organoid models, progressively enhancing their capacity to replicate the complex microenvironment of NVU. The permeability of *in vitro* BBB models is evaluated by measuring P_{app} and TEER. At the *in vivo* level, imaging technologies complement one another to establish a comprehensive system for real-time, non-invasive assessment of BBB permeability.

To overcome the limitations of existing technologies in terms of physiological relevance, dynamic monitoring capabilities, and quantitative accuracy, future BBB permeability assessment technologies will exhibit a distinct trend toward multimodal integration and intelligence-driven strategies. On the one hand, *in vitro* model systems will evolve from "simple simulation" to "precision recapitulation": patient-specific organ-on-a-chip and organoid technologies will achieve highly biomimetic reconstruction of NVU, closely mimicking the human physiological environment. The integration of high-throughput barrier assessment, transporter functional analysis, and multi-omics technologies will enable multidimensional characterization of functional phenotypes. On the other hand, *in vivo* imaging will use high-resolution MRI, novel PET probes, and NIR-II optical imaging to achieve non-invasive, dynamic, quantitative monitoring of BBB permeability.

AI will become the core driver of this paradigm. By integrating multi-omics data, simulating molecular–barrier interactions, and optimizing drug design—such as using deep learning to predict compound permeability or intelligently identifying barrier damage features from imaging data—AI will fundamentally reshape BBB permeability research. The deep integration of AI will establish a closed loop of "computational prediction — *in vitro* validation — *in vivo* confirmation," not only dramatically enhancing drug screening efficiency but also enabling the mechanistic interpretation and dynamic prediction of BBB function through multi-omics data integration. Furthermore, the deep application of AI in image processing will enable the automatic and quantitative extraction of critical information—such as leakage characteristics and vascular network morphology—from vast optical imaging datasets. This advancement will bridge the gap between mere observation and comprehensive understanding and predictive capabilities. These developments will significantly enhance our ability to perform dynamic, holistic analyses of the functional state of the BBB in living organisms, ultimately driving innovation in diagnostic approaches and therapeutic strategies for CNS disorders.

Acknowledgement

This study was supported by the National Key Research and Development Program of China (2023YFF0724100), National Natural Science Foundation of China (22393934, 22274097).

Author contributions

Yanhong SUN, Shihua LUO, Ying Zhu and Miaomiao WANG conceived, designed, discussed the work and revised the manuscript. Lu GAN, Miaomiao WANG and Yiru FAN edited the manuscript. Miaomiao WANG and Chenxi Duan prepared figures. All authors have read and approved the final manuscript.

Compliance with ethics guidelines

This review does not contain any studies with human or animal subjects performed by any of the authors.

Declaration on the use of generative AI tools

In preparing this work, the authors used Deepseek to refine language and grammar, and Doubao to improve artwork visual quality (e.g., resolution and color correction). The authors reviewed and edited the output and take full responsibility for the final content.

References

Ahlawat J, Barroso GG, Asil SM, et al., 2020. Nanocarriers as potential drug delivery candidates for overcoming the blood-brain barrier: Challenges and possibilities. *ACS Omega*, 5(22):12583-12595. https://doi.org/10.1021/acsomega.0c01592

Ambudkar SV, Dey S, Hrycyna CA, et al., 1999. Biochemical, cellular, and pharmacological aspects of the multidrug transporter. *Annu Rev Pharmacol Toxicol*, 39(1):361-398. https://doi.org/10.1146/annurev.pharmtox.39.1.361

Anderson JM, Van Itallie CM, 2009. Physiology and function of the tight junction. *Cold Spring Harb Perspect Biol*, 1(2):a002584 https://doi.org/10.1101/cshperspect.a002584

Appelt-Menzel A, Cubukova A, Günther K, et al., 2017. Establishment of a human blood-brain barrier co-culture model mimicking the neurovascular unit using induced pluri- and multipotent stem cells. *Stem Cell Rep*, 8(4):894-906. https://doi.org/10.1016/j.stemcr.2017.02.021

Badiola-Mateos M, Di Giuseppe D, Paoli R, et al., 2021. A novel multi-frequency trans-endothelial electrical resistance (mteer) sensor array to monitor blood-brain barrier integrity. *Sens Actuators B: Chem*, 334:129599. https://doi.org/10.1016/j.snb.2021.129599

Bagchi S, Chhibber T, Lahooti B, et al., 2019. In-vitro blood-brain barrier models for drug screening and permeation studies: An overview. *Drug Des Devel Ther*, 13:3591-3605. https://doi.org/10.2147/dddt.s218708

Balzer V, Poc P, Puris E, et al., 2022. Re-evaluation of the hCMEC/D3 based bbb model for abc transporter studies. *Eur J Pharm Biopharm*, 173:12-21. https://doi.org/10.1016/j.ejpb.2022.02.017

Banerjee J, Shi Y, Azevedo HS, 2016. *In vitro* blood–brain barrier models for drug research: State-of-the-art and new perspectives on reconstituting these models on artificial basement membrane platforms. *Drug Discov Today*, 21(9):1367-1386. https://doi.org/10.1016/j.drudis.2016.05.020

Banks WA, 2016. From blood-brain barrier to blood-brain interface: New opportunities for cns drug delivery. *Nat Rev Drug Discovery*, 15(4):275-292. https://doi.org/10.1038/nrd.2015.21

Bauer M, Karch R, Zeitlinger M, et al., 2014. *In vivo* p-glycoprotein function before and after epilepsy surgery. *Neurology*, 83(15):1326-1331. https://doi.org/10.1212/WNL.0000000000000858

Bayir E, Celtikoglu MM, Sendemir A, 2019. The use of bacterial cellulose as a basement membrane improves the plausibility of the static blood-brain barrier model. *Int J Biol Macromol*, 126:1002-1013. https://doi.org/10.1016/j.ijbiomac.2018.12.257

Bell RD, Winkler EA, Sagare AP, et al., 2010. Pericytes control key neurovascular functions and neuronal phenotype in the adult brain and during brain aging. *Neuron*, 68(3):409-427. https://doi.org/10.1016/j.neuron.2010.09.043

Benson K, Cramer S, Galla HJ, 2013. Impedance-based cell monitoring: Barrier properties and beyond. *Fluids Barriers CNS*, 10(1):5. https://doi.org/10.1186/2045-8118-10-5

Bergmann S, Lawler SE, Qu Y, et al., 2018. Blood–brain-barrier organoids for investigating the permeability of cns therapeutics. *Nat Protoc*, 13(12):2827-2843.

https:/doi.org/10.1038/s41596-018-0066-x

Bhalerao A, Sivandzade F, Archie SR, et al., 2020. *In vitro* modeling of the neurovascular unit: Advances in the field. *Fluids Barriers CNS*, 17(1):22. https://doi.org/10.1186/s12987-020-00183-7

Bhattacharya A, Kaushik DK, Lozinski BM, et al., 2020. Beyond barrier functions: Roles of pericytes in homeostasis and regulation of neuroinflammation. *J Neurosci Res*, 98(12):2390-2405. https://doi.org/10.1002/jnr.24715

Cao J, Zhu B, Zheng K, et al., 2020. Recent progress in NIR-II contrast agent for biological imaging. *Front Bioeng Biotechnol*, 7:487. https://doi.org/10.3389/fbioe.2019.00487

Cao PY, He Y, Cui MY, et al., 2024. Group graph: A molecular graph representation with enhanced performance, efficiency and interpretability. *J Cheminform*, 16(1):133. https://doi.org/10.1186/s13321-024-00933-x

Ceccarelli MC, Lefevre MC, Marino A, et al., 2024. Real-time monitoring of a 3D blood–brain barrier model maturation and integrity with a sensorized microfluidic device. *Lab Chip*, 24(22):5085-5100. https://doi.org/10.1039/d4lc00633j

Cecchelli R, Berezowski V, Lundquist S, et al., 2007. Modelling of the blood–brain barrier in drug discovery and development. *Nat Rev Drug Discovery*, 6(8):650-661. https://doi.org/10.1038/nrd2368

Chen H, Tong X, Lang L, et al., 2017. Quantification of tumor vascular permeability and blood volume by positron emission tomography. *Theranostics*, 7(9):2363. https://doi.org/10.7150/thno.19898

Chen H, Mirg S, Gaddale P, et al., 2024a. Multiparametric brain hemodynamics imaging using a combined ultrafast ultrasound and photoacoustic system. *Adv Sci*, 11(31):2401467. https://doi.org/10.1002/advs.202401467

Chen X, Xu J, Guo S, et al., 2024b. Blood-brain barrier permeability by ct perfusion predicts parenchymal hematoma after recanalization with thrombectomy. *J Neuroimaging*, 34(2):241-248. https://doi.org/10.1111/jon.13172

Chen X, Kang D, Han Z, et al., 2025. Prognostic value of tumor infiltrating lymphocytes in luminal b breast cancer based on multiphoton microscopy. *J Biophotonics*, :e202500281. https://doi.org/10.1002/jbio.202500281

Chung B, Kim J, Nam J, et al., 2020. Evaluation of cell-penetrating peptides using microfluidic *in vitro* 3D brain endothelial barrier. *Macromol Biosci*, 20(6):1900425. https://doi.org/10.1002/mabi.201900425

Chung KJ, Abdelhafez YG, Spencer BA, et al., 2025. Quantitative pet imaging and modeling of molecular blood-brain barrier permeability. *Nat Commun*, 16(1):3076. https://doi.org/10.1038/s41467-025-58356-7

Clark DE, 2003. *In silico* prediction of blood–brain barrier permeation. *Drug Discov Today*, 8(20):927-933. https://doi.org/10.1016/S1359-6446(03)02827-7

Cornford EM, Hyman S, 1999. Blood–brain barrier permeability to small and large molecules. *Adv Drug Deliv Rev*, 36(2-3):145-163. https://doi.org/10.1016/S0169-409X(98)00082-9

Cucullo L, Couraud PO, Weksler B, et al., 2008. Immortalized human brain endothelial cells and flow-based vascular modeling: A marriage of convenience for rational neurovascular studies. *J Cereb Blood Flow Metab*, 28(2):312-328. https://doi.org/10.1038/sj.jcbfm.9600525

Cucullo L, Marchi N, Hossain M, et al., 2011. A dynamic *in vitro* BBB model for the study of immune cell trafficking into the central nervous system. *J Cereb Blood Flow Metab*, 31(2):767-777. https://doi.org/10.1038/jcbfm.2010.162

Dai J, Wei W, Yan C, et al., 2025. Multiplex imaging of amyloid-β plaques dynamics in living brains with quinoline-malononitrile-based probes. *Nat Biomed Eng*, 9(10):1632-1644. https://doi.org/10.1038/s41551-025-01392-x

Daniels BP, Cruz-Orengo L, Pasieka TJ, et al., 2013. Immortalized human cerebral microvascular endothelial cells maintain the properties of primary cells in an *in vitro* model of immune migration across the blood brain barrier. *J Neurosci Methods*, 212(1):173-179. https://doi.org/10.1016/j.jneumeth.2012.10.001

Dao L, You Z, Lu L, et al., 2024. Modeling blood-brain barrier formation and cerebral cavernous malformations in human

psc-derived organoids. *Cell Stem Cell*, 31(6):818-833. e811.
https://doi.org/10.1016/j.stem.2024.04.019

De Klerk OL, Willemsen AT, Roosink M, et al., 2009. Locally increased p-glycoprotein function in major depression: A pet study with [11c] verapamil as a probe for p-glycoprotein function in the blood–brain barrier. *Int J Neuropsychopharmacol*, 12(7):895-904.
https://doi.org/10.1017/s1461145709009894

De Vivo DC, Trifiletti RR, Jacobson RI, et al., 1991. Defective glucose transport across the blood-brain barrier as a cause of persistent hypoglycorrhachia, seizures, and developmental delay. *N Engl J Med*, 325(10):703-709.
https://doi.org/10.1056/nejm199109053251006

Deli MA, Ábrahám CS, Kataoka Y, et al., 2005. Permeability studies on *in vitro* blood–brain barrier models: Physiology, pathology, and pharmacology. *Cell Mol Neurobiol*, 25(1):59-127.
https://doi.org/10.1007/s10571-004-1377-8

Denk W, Strickler JH, Webb WW, 1990. Two-photon laser scanning fluorescence microscopy. *Science*, 248(4951):73-76.
https://doi.org/10.1126/science.2321027

Dey V, Ning X, 2024. Enhancing molecular property prediction with auxiliary learning and task-specific adaptation. *J Cheminform*, 16(1):85.
https://doi.org/10.1186/s13321-024-00880-7

Di L, Rong H, Feng B, 2013. Demystifying brain penetration in central nervous system drug discovery: Miniperspective. *J Med Chem*, 56(1):2-12.
https://doi.org/10.1021/jm301297f

Dohgu S, Takata F, Yamauchi A, et al., 2005. Brain pericytes contribute to the induction and up-regulation of blood–brain barrier functions through transforming growth factor-β production. *Brain Res*, 1038(2):208-215.
https://doi.org/10.1016/j.brainres.2005.01.027

Dong XW, 2018. Current strategies for brain drug delivery. *Theranostics*, 8(6):1481-1493.
https://doi.org/10.7150/thno.21254

Douville NJ, Tung Y-C, Li R, et al., 2010. Fabrication of two-layered channel system with embedded electrodes to measure resistance across epithelial and endothelial barriers. *Anal Chem*, 82(6):2505-2511.
https://doi.org/10.1021/ac9029345

Elbaz M, Ad-El N, Chulanova Y, et al., 2025. Low-frequency ultrasound-mediated blood-brain barrier opening enables non-invasive lipid nanoparticle rna delivery to glioblastoma. *J Control Release,* 385:114018.
https://doi.org/10.1016/j.jconrel.2025.114018

Feldmann M, Asselin M-C, Liu J, et al., 2013. P-glycoprotein expression and function in patients with temporal lobe epilepsy: A case-control study. *Lancet Neurol*, 12(8):777-785.
https://doi.org/10.1016/s1474-4422(13)70109-1

Fernández-Seara MA, Wang Z, Wang J, et al., 2005. Continuous arterial spin labeling perfusion measurements using single shot 3D grase at 3 t. *Magn Reson Med*, 54(5):1241-1247.
https://doi.org/10.1002/mrm.20674

Franke H, Galla HJ, Beuckmann CT, 1999. An improved low-permeability *in vitro*-model of the blood–brain barrier: Transport studies on retinoids, sucrose, haloperidol, caffeine and mannitol. *Brain Res*, 818(1):65-71.
https://doi.org/10.1016/S0006-8993(98)01282-7

Grant N, Machado Reyes D, Yang Z, et al., 2025. Blood brain barrier permeability prediction with artificial intelligence and machine learning: A meta-review and future directions. *Discov Artif Intell*, 5(1):254.
https://doi.org/10.1007/s44163-025-00494-4

Grkovski R, Acu L, Ahmadli U, et al., 2023a. Dual-energy computed tomography in stroke imaging: Value of a new image acquisition technique for ischemia detection after mechanical thrombectomy. *Clin Neuroradiol*, 33(3):747-754.
https://doi.org/10.1007/s00062-023-01270-6

Grkovski R, Acu L, Ahmadli U, et al., 2023b. A novel dual-energy ct method for detection and differentiation of intracerebral hemorrhage from contrast extravasation in stroke patients after endovascular thrombectomy: Feasibility and first results. *Clini Neuroradiol*, 33(1):171-177.
https://doi.org/10.1007/s00062-022-01198-3

Hajal C, Offeddu GS, Shin Y, et al., 2022. Engineered human blood–brain barrier microfluidic model for vascular permeability analyses. *Nat Protoc*, 17(1):95-128.
https://doi.org/10.1038/s41596-021-00635-w

Harilal S, Jose J, Parambi DT, et al., 2020. Revisiting the blood-brain barrier: A hard nut to crack in the transportation of drug molecules. *Brain Res Bull*, 160:121-140.
https://doi.org/10.1016/j.brainresbull.2020.03.018

He QG, Liu J, Liang J, et al., 2018. Towards improvements for penetrating the blood-brain barrier-recent progress from a material and pharmaceutical perspective. *Cells*, 7(4):24. https://doi.org/10.3390/cells7040024

Heye AK, Culling RD, Hernández MDCV, et al., 2014. Assessment of blood–brain barrier disruption using dynamic contrast-enhanced MRI. A systematic review. *Neuroimage Clin,* 6:262-274. https://doi.org/10.1016/j.nicl.2014.09.002

Hong G, Lee JC, Robinson JT, et al., 2012. Multifunctional *in vivo* vascular imaging using near-infrared ii fluorescence. *Nat Med*, 18(12):1841-1846. https://doi.org/10.1038/nm.2995

Hong G, Antaris AL, Dai H, 2017. Near-infrared fluorophores for biomedical imaging. *Nat Biomed Eng*, 1(1):0010. https://doi.org/10.1038/s41551-016-0010

Hui J, Li R, Phillips EH, et al., 2016. Bond-selective photoacoustic imaging by converting molecular vibration into acoustic waves. *Photoacoustics*, 4(1):11. https://doi.org/10.1016/j.pacs.2016.01.002

Hurst R, Fritz I, 1996. Properties of an immortalised vascular endothelial/glioma cell co-culture model of the blood-brain barrier. *J Cell Physiol*, 167(1):81-88. https://doi.org/10.1002/(SICI)1097-4652(199604)167:1<81::AID-JCP9>3.0.CO;2-8

Iliff JJ, Wang MH, Liao YH, et al., 2012. A paravascular pathway facilitates csf flow through the brain parenchyma and the clearance of interstitial solutes, including amyloid β. *Sci Transl Med*, 4(147):147ra111. https://doi.org/10.1126/scitranslmed.3003748

Ito R, Umehara K, Suzuki S, et al., 2019. A human immortalized cell-based blood brain barrier triculture model: Development and characterization as a promising tool for drug-brain permeability studies. *Mol Pharm*, 16(11):4461-4471. https://doi.org/10.1021/acs.molpharmaceut.9b00519

Jackson I, Luo A, Webb E, et al., 2021. A new *in silico* approach to revolutionize cns pet tracer design and enhance translational success. *Nucl Med Biol*, 96:S24-S25. https://doi.org/10.1016/S0969-8051(21)00304-8

Janigro D, Leaman SM, Stanness KA, 1999. Dynamic *in vitro* modeling of the blood–brain barrier: A novel tool for studies of drug delivery to the brain. *Pharm Sci Technol Today*, 2(1):7-12. https://doi.org/10.1016/s1461-5347(98)00110-2

Jiang D, Wu Z, Hsieh CY, et al., 2021. Could graph neural networks learn better molecular representation for drug discovery? A comparison study of descriptor-based and graph-based models. *J Cheminform*, 13(1):12. https://doi.org/10.1186/s13321-020-00479-8

Jiang L, Li S, Zheng J, et al., 2019. Recent progress in microfluidic models of the blood-brain barrier. *Micromachines*, 10(6):375. https://doi.org/10.3390/mi10060375

Johnson TR, Krauss B, Sedlmair M, et al., 2007. Material differentiation by dual energy ct: Initial experience. *Eur Radiol*, 17(6):1510-1517. https://doi.org/10.1007/s00330-006-0517-6

Juliano RL, Ling V, 1976. A surface glycoprotein modulating drug permeability in chinese hamster ovary cell mutants. *Biochim Biophys Acta (BBA)-Biomembr*, 455(1):152-162. https://doi.org/10.1016/0005-2736(76)90160-7

Kadry H, Noorani B, Cucullo L, 2020. A blood-brain barrier overview on structure, function, impairment, and biomarkers of integrity. *Fluids Barriers CNS*, 17(1):69. https://doi.org/10.1186/s12987-020-00230-3

Kisler K, Nelson AR, Rege SV, et al., 2017. Pericyte degeneration leads to neurovascular uncoupling and limits oxygen supply to brain. *Nat Neurosci*, 20(3):406-416. https://doi.org/10.1038/nn.4489

Krol S, Macrez R, Docagne F, et al., 2013. Therapeutic benefits from nanoparticles: The potential significance of nanoscience in diseases with compromise to the blood brain barrier. *Chem Rev*, 113(3):1877-1903. https://doi.org/10.1021/cr200472g

Lee S, Kang BM, Kim JH, et al., 2018. Real-time *in vivo* two-photon imaging study reveals decreased cerebro-vascular volume and increased blood-brain barrier permeability in chronically stressed mice. *Sci Rep*, 8(1):13064. https://doi.org/10.1038/s41598-018-30875-y

Li J, Wang T, Zhang X, et al., 2025a. Chalcogenapyrylium-engineered d-π-a probe for enhanced optoacoustic imaging of amyloid-β plaques. *Sens Actuators B: Chem*, 442:138086. https://doi.org/10.1016/j.snb.2025.138086

Li W, Sun X, Wang Y, et al., 2014. *In vivo* quantitative photoacoustic microscopy of gold nanostar kinetics in mouse organs.

Biomed Opt Express, 5(8):2679-2685. https://doi.org/10.1364/BOE.5.002679

Li W, Zha X, Zhang X, et al., 2025b. Enhanced positron emission tomography imaging of β-amyloid through focused ultrasound-mediated gallium-68 radiotracer delivery across the blood-brain barrier. *ACS Chem Neurosci*, 16(15):3070-3081. https://doi.org/10.1016/j.snb.2025.138086

Li X, Fourches D, 2020. Inductive transfer learning for molecular activity prediction: Next-gen qsar models with molpmofit. *J Cheminform*, 12(1):27. https://doi.org/10.1186/s13321-020-00430-x

Lin L, Wang LV, 2022. The emerging role of photoacoustic imaging in clinical oncology. *Nat Rev Clin Oncol*, 19(6):365-384. https://doi.org/10.1038/s41571-022-00615-3

Lin Z, Li Y, Su P, et al., 2018. Non-contrast mr imaging of blood-brain barrier permeability to water. *Magn Reson Med*, 80(4):1507-1520. https://doi.org/10.1002/mrm.27141

Liu JJ, Wang T, Dong J, et al., 2025. The blood-brain barriers: Novel nanocarriers for central nervous system diseases. *J Nanobiotechnol*, 23(1):29. https://doi.org/10.1186/s12951-025-03247-8

Liu L, Zhang L, Feng H, et al., 2021. Prediction of the blood–brain barrier (bbb) permeability of chemicals based on machine-learning and ensemble methods. *Chem Res Toxicol*, 34(6):1456-1467. https://doi.org/10.1021/acs.chemrestox.0c00343

Liu P, Uh J, Lu H, 2011. Determination of spin compartment in arterial spin labeling mri. *Magn Reson Med*, 65(1):120-127. https://doi.org/10.1002/mrm.22601

Liu X, Duan Y, Liu B, 2021. Nanoparticles as contrast agents for photoacoustic brain imaging. *Aggregate*, 2(1):4-19. https://doi.org/10.1002/agt2.26

Logan S, Arzua T, Canfield SG, et al., 2019. Studying human neurological disorders using induced pluripotent stem cells: From 2d monolayer to 3D organoid and blood brain barrier models. *Compr Physiol*, 9(2):565-611. https://doi.org/10.1002/j.2040-4603.2019.tb00076.x

Löscher W, Friedman A, 2020. Structural, molecular, and functional alterations of the blood-brain barrier during epileptogenesis and epilepsy: A cause, consequence, or both? *Int J Mol Sci*, 21(2):591. https://doi.org/10.3390/ijms21020591

Lu C, Meng C, Li Y, et al., 2024. A probe for NIR-II imaging and multimodal analysis of early alzheimer's disease by targeting ctgf. *Nat Commun*, 15(1):5000. https://doi.org/10.1038/s41467-024-49409-4

Luissint AC, Artus C, Glacial F, et al., 2012. Tight junctions at the blood brain barrier: Physiological architecture and disease-associated dysregulation. *Fluids Barriers CNS*, 9(1):23. https://doi.org/10.1186/2045-8118-9-23

Malik M, Steele SA, Mitra D, et al., 2025. Trans-epithelial/endothelial electrical resistance (TEER): Current state of integrated TEER measurements in organ-on-a-chip devices. *Curr Opin Biomed Eng*, 34:100588. https://doi.org/10.1016/j.cobme.2025.100588

Malinova TS, Huveneers S, 2018. Sensing of cytoskeletal forces by asymmetric adherens junctions. *Trends Cell Biol*, 28(4):328-341. https://doi.org/https://doi.org/10.1016/j.tcb.2017.11.002

Mantecón-Oria M, Diban N, Berciano MT, et al., 2020. Hollow fiber membranes of pcl and pcl/graphene as scaffolds with potential to develop *in vitro* blood—brain barrier models. *Membranes*, 10(8):161. https://doi.org/10.3390/membranes10080161

Mantecón-Oria M, Rivero MJ, Diban N, et al., 2022a. On the quest of reliable 3D dynamic *in vitro* blood-brain barrier models using polymer hollow fiber membranes: Pitfalls, progress, and future perspectives. *Front Bioeng Biotechnol*, 10:1056162. https://doi.org/10.3389/fbioe.2022.1056162

Mantecón-Oria M, Tapia O, Lafarga M, et al., 2022b. Influence of the properties of different graphene-based nanomaterials dispersed in polycaprolactone membranes on astrocytic differentiation. *Sci Rep*, 12(1):13408. https://doi.org/10.1038/s41598-022-17697-9

Mantecón-Oria M, Rivero MJ, Löscher W, et al., 2025. Breaking optical barriers: Transparent polymeric hollow fibers for biomedical applications. *View*, :20250076. https://doi.org/10.1002/VIW.20250076

Mármol I, Abizanda-Campo S, Ayuso JM, et al., 2023. Towards novel biomimetic *in vitro* models of the blood–brain barrier for drug permeability evaluation. *Bioengineering*, 10(5):572. https://doi.org/10.3390/bioengineering10050572

Mensch J, Oyarzabal J, Mackie C, et al., 2009. *In vivo*, *in vitro* and *in silico* methods for small molecule transfer across the bbb. *J Pharm Sci*, 98(12):4429-4468. https://doi.org/10.1002/jps.21745

Miles KA, Griffiths M, 2003. Perfusion ct: A worthwhile enhancement? *Br J Radiol*, 76(904):220-231. https://doi.org/10.1259/bjr/13564625

Mouchtouris N, Ailes I, Gooch R, et al., 2024. Quantifying blood-brain barrier permeability in patients with ischemic stroke using non-contrast mri. *Magn Reson Imaging*, 109:165-172. https://doi.org/10.1016/j.mri.2024.03.027

Muruganandam A, Herx LM, Monette R, et al., 1997. Development of immortalized human cerebromicrovascular endothelial cell line as an *in vitro* model of the human blood–brain barrier. *FASEB J*, 11(13):1187-1197. https://doi.org/10.1096/fasebj.11.13.9367354

Naik P, Cucullo L, 2012. *In vitro* blood–brain barrier models: Current and perspective technologies. *J Pharm Sci*, 101(4):1337-1354. https://doi.org/10.1002/jps.23022

Nakagawa S, Deli MA, Kawaguchi H, et al., 2009. A new blood–brain barrier model using primary rat brain endothelial cells, pericytes and astrocytes. *Neurochem Int*, 54(3-4):253-263. https://doi.org/10.1016/j.neuint.2008.12.002

Nation DA, Sweeney MD, Montagne A, et al., 2019. Blood–brain barrier breakdown is an early biomarker of human cognitive dysfunction. *Nat Med*, 25(2):270-276. https://doi.org/10.1038/s41591-018-0297-y

Nazari H, Shrestha J, Naei VY, et al., 2023. Advances in TEER measurements of biological barriers in microphysiological systems. *Biosens Bioelectron*, 234:115355. https://doi.org/10.1016/j.bios.2023.115355

Neuhaus W, Lauer R, Oelzant S, et al., 2006. A novel flow based hollow-fiber blood–brain barrier *in vitro* model with immortalised cell line pbmec/c1–2. *J Biotechnol*, 125(1):127-141. https://doi.org/10.1016/j.jbiotec.2006.02.019

Nogueira DE, Cabral JM,Rodrigues CA, 2021. Single-use bioreactors for human pluripotent and adult stem cells: Towards regenerative medicine applications. *Bioengineering*, 8(5):68. https://doi.org/10.3390/bioengineering8050068

Nzou G, Wicks R, Wicks E, et al., 2018. Human cortex spheroid with a functional blood brain barrier for high-throughput neurotoxicity screening and disease modeling. *Sci Rep*, 8(1):7413. https://doi.org/10.1038/s41598-018-25603-5

Ogunshola OO, 2011. *In vitro* modeling of the blood-brain barrier: Simplicity versus complexity. *Curr Pharm Des*, 17(26):2755-2761. https://doi.org/10.2174/138161211797440159

Oddo A, Peng B, Tong Z, et al., 2019. Advances in microfluidic blood–brain barrier (bbb) models. *Trends Biotechnol*, 37(12):1295-1314. https://doi.org/10.1016/j.tibtech.2019.04.006

Pandit R, Chen LY, Götz J, 2020. The blood-brain barrier: Physiology and strategies for drug delivery. *Adv Drug Deliv Rev*, 165-166:1-14. https://doi.org/10.1016/j.addr.2019.11.009

Pardridge WM, 2005. The blood-brain barrier: Bottleneck in brain drug development. *Neurorx*, 2(1):3-14. https://doi.org/10.1602/neurorx.2.1.3

Parkes LM, Tofts PS, 2002. Improved accuracy of human cerebral blood perfusion measurements using arterial spin labeling: Accounting for capillary water permeability. *Magn Reson Med*, 48(1):27-41. https://doi.org/10.1002/mrm.10180

Poon CT, Shah K, Lin C, et al., 2018. Time course of focused ultrasound effects on β-amyloid plaque pathology in the tgcrnd8 mouse model of alzheimer's disease. *Sci Rep*, 8(1):14061. https://doi.org/10.1038/s41598-018-32250-3

Qin W, Li H, Chen J, et al., 2025. Amphiphilic hemicyanine molecular probes crossing the blood-brain barrier for intracranial optical imaging of glioblastoma. *Sci Adv*, 11(3):eadq5816. https://doi.org/10.1126/sciadv.adq5816

Qiu Y, Li H, Yu K, et al., 2025. Collagen fibers quantification for liver fibrosis assessment using linear dichroism photoacoustic microscopy. *Photoacoustics*, 42:100694. https://doi.org/10.1016/j.pacs.2025.100694

Raja R, Rosenberg GA, Caprihan A, 2018. Mri measurements of blood-brain barrier function in dementia: A review of recent

studies. *Neuropharmacology*, 134:259-271.
https://doi.org/10.1016/j.neuropharm.2017.10.034

Rollins ZA, Cheng AC, Metwally E, 2024. Molprop: Molecular property prediction with multimodal language and graph fusion. *J Cheminform*, 16(1):56.
https://doi.org/10.1186/s13321-024-00846-9

Rubin L, Hall D, Porter S, et al., 1991. A cell culture model of the blood-brain barrier. *J Cell Biol*, 115(6):1725-1735.
https://doi.org/10.1083/jcb.115.6.1725

Salehi Farid A, Rowley JE, Allen HH, et al., 2025. Cd45-pet is a robust, non-invasive tool for imaging inflammation. *Nature*, 639(8053):214-224.
https://doi.org/10.1038/s41586-024-08441-6

Saxena D, Sharma A, Siddiqui MH, et al., 2019. Blood brain barrier permeability prediction using machine learning techniques: An update. *Curr Pharm Biotechnol,* 20(14):1163-1171.
https://doi.org/10.2174/1389201020666190821145346

Schurhoff N, Toborek M, 2023. Circadian rhythms in the blood-brain barrier: Impact on neurological disorders and stress responses. *Mol Brain*, 16(1):5.
https://doi.org/10.1186/s13041-023-00997-0

Segarra M, Aburto MR, Acker-Palmer A, 2021. Blood-brain barrier dynamics to maintain brain homeostasis. *Trends Neurosci*, 44(5):393-405.
https://doi.org/10.1016/j.tins.2020.12.002

Shaker B, Yu MS, Song JS, et al., 2021. Lightbbb: Computational prediction model of blood–brain-barrier penetration based on lightgbm. *Bioinformatics*, 37(8):1135-1139.
https://doi.org/10.1093/bioinformatics/btaa918

Shang B, Wang T, Zhao S, et al., 2024. Higher blood-brain barrier permeability in patients with major depressive disorder identified by dce-mri imaging. *Psychiatry Res Neuroimaging*, 337:111761.
https://doi.org/10.1016/j.pscychresns.2023.111761

Siegel MJ, Kaza RK, Bolus DN, et al., 2016. White paper of the society of computed body tomography and magnetic resonance on dual-energy ct, part 1: Technology and terminology. *J Comput Assist Tomogr*, 40(6):841-845.
https://doi.org/10.1097/rct.0000000000000531

Simonneau C, Duschmalé M, Gavrilov A, et al., 2021. Investigating receptor-mediated antibody transcytosis using blood–brain barrier organoid arrays. *Fluids Barriers CNS*, 18(1):43.
https://doi.org/10.1186/s12987-021-00276-x

Sivandzade F, Cucullo L, 2018. In-vitro blood-brain barrier modeling: A review of modern and fast-advancing technologies. *J Cereb Blood Flow Metab*, 38(10):1667-1681.
https://doi.org/10.1177/0271678x18788769

Sonninen TM, Peltonen S, Kälvälä S, et al., 2025. From inserts to chips: Microfluidic culture and 3D astrocyte co-culture drive functional and transcriptomic changes in hipsc-derived endothelial cells. *Fluids Barriers CNS*, 22(1):58.
https://doi.org/10.1186/s12987-025-00672-7

Srinivasan B, Kolli AR, Esch MB, et al., 2015. TEER measurement techniques for *in vitro* barrier model systems. *J Lab Autom*, 20(2):107-126.
https://doi.org/10.1177/2211068214561025

Srinivasan B, Kolli AR, 2018. Transepithelial/transendothelial electrical resistance (TEER) to measure the integrity of blood-brain barrier. *Blood-Brain Barrier, Springer*, 99-114.
https://doi.org/10.1007/978-1-4939-8946-1_6

Srinivasan B, Kolli AR, 2025. Transepithelial/transendothelial electrical resistance (TEER) to measure the integrity of blood-brain barrier. *Springer* , 127-144.
https://doi.org/10.1007/978-1-0716-4474-4_8

St. Lawrence K, Frank J, Mclaughlin A, 2000. Effect of restricted water exchange on cerebral blood flow values calculated with arterial spin tagging: A theoretical investigation. *Magnetic Resonance in Medicine: Magn Reson Med,* 44(3):440-449.
https://doi.org/10.1002/1522-2594(200009)44:3<440::AID-MRM15>3.0.CO;2-6

St. Lawrence KS, Owen D, Wang DJ, 2012. A two-stage approach for measuring vascular water exchange and arterial transit time by diffusion-weighted perfusion mri. *Magn Reson Med*, 67(5):1275-1284.
https://doi.org/10.1002/mrm.23104

Stamatovic SM, Johnson AM, Keep RF, et al., 2016. Junctional proteins of the blood-brain barrier: New insights into function and dysfunction. *Tissue Barriers*, 4(1):e1154641.
https://doi.org/10.1080/21688370.2016.1154641

Stanness KA, Westrum LE, Fornaciari E, et al., 1997. Morphological and functional characterization of an *in vitro* blood–brain

barrier model. *Brain Res*, 771(2):329-342.
https://doi.org/10.1016/S0006-8993(97)00829-9

Sun J, Song S, 2024. Advances in modeling permeability and selectivity of the blood-brain barrier using microfluidics. *Microfluid Nanofluidics*, 28(7):44.
https://doi.org/10.1007/s10404-024-02741-z

Tevosyan A, Khondkaryan L, Khachatrian H, et al., 2022. Improving vae based molecular representations for compound property prediction. *J Cheminform,* 14(1):69.
https://doi.org/10.1186/s13321-022-00648-x

Toyohara J, 2016. Importance of p-gp pet imaging in pharmacology. *Curr Pharm Des*, 22(38):5830-5836.
https://doi.org/10.2174/1381612822666160804092258

Tu KH, Yu LS, Sie ZH, et al., 2020. Development of real-time transendothelial electrical resistance monitoring for an *in vitro* blood-brain barrier system. *Micromachines*, 12(1):37.
https://doi.org/10.3390/mi12010037

Turowski P, Kenny BA, 2015. The blood-brain barrier and methamphetamine: Open sesame? *Front Neurosci*, 9:156.
https://doi.org/10.3389/fnins.2015.00156

Van De Haar HJ, Burgmans S, Jansen JF, et al., 2016. Blood-brain barrier leakage in patients with early alzheimer disease. *Radiology*, 281(2):527-535.
https://doi.org/10.1148/radiol.2016152244

Van Der Helm MW, Odijk M, Frimat J-P, et al., 2016. Direct quantification of transendothelial electrical resistance in organs-on-chips. *Biosens Bioelectron*, 85:924-929.
https://doi.org/10.1016/j.bios.2016.06.014

Verstappen D, De Jong JJ, Voorter PH, et al., 2025. Dce-mri reveals spatial pattern in heterogeneous blood-brain barrier leakage within white matter in cerebral small vessel disease. *J Cereb Blood Flow Metab*, 45(11):2104-2114.
https://doi.org/10.1177/0271678x251364151

Vigh JP, Kincses A, Ozgür B, et al., 2021. Transendothelial electrical resistance measurement across the blood–brain barrier: A critical review of methods. *Micromachines*, 12(6):685.
https://doi.org/10.3390/mi12060685

Vorbrodt AW, Dobrogowska DH, 2003. Molecular anatomy of intercellular junctions in brain endothelial and epithelial barriers: Electron microscopist's view. *Brain Res Rev*, 42(3):221-242.
https://doi.org/10.1016/S0165-0173(03)00177-2

Wang D, Chen FL, Han ZL, et al., 2021. Relationship between amyloid-β deposition and blood-brain barrier dysfunction in alzheimer's disease. *Front Cell Neurosci*, 15:695479.
https://doi.org/10.3389/fncel.2021.695479

Wang G, Zhou Y, Yu C, et al., 2024. Intravital photoacoustic brain stimulation with high-precision. *J Biomed Opt*, 29(S1):S11520-S11520.
https://doi.org/10.1117/1.jbo.29.s1.s11520

Wang J, Fernández-Seara MA, Wang S, et al., 2007. When perfusion meets diffusion: *In vivo* measurement of water permeability in human brain. *J Cereb Blood Flow Metab*, 27(4):839-849.
https://doi.org/10.1038/sj.jcbfm.9600398

Wang S, Shi H, Wang L, et al., 2022. Photostable small-molecule NIR-II fluorescent scaffolds that cross the blood–brain barrier for noninvasive brain imaging. *J Am Chem Soc*, 144(51):23668-23676.
https://doi.org/10.1021/jacs.2c11223

Wang X, Li P, Ding Q, et al., 2019. Observation of acetylcholinesterase in stress-induced depression phenotypes by two-photon fluorescence imaging in the mouse brain. *J Am Chem Soc*, 141(5):2061-2068.
https://doi.org/10.1021/jacs.8b11414

Wang X, Hou Y, Ai X, et al., 2020. Potential applications of microfluidics based blood brain barrier (BBB)-on-chips for *in vitro* drug development. *Biomed Pharmacother*, 132:110822.
https://doi.org/10.1016/j.biopha.2020.110822

Weksler B, Romero IA, Couraud PO, 2013. The hCMEC/D3 cell line as a model of the human blood brain barrier. *Fluids Barriers CNS*, 10(1):16.
https://doi.org/10.1186/2045-8118-10-16

Wen N, Liu G, Zhang J, et al., 2022. A fingerprints based molecular property prediction method using the bert model. *J Cheminform,* 14(1):71.
https://doi.org/10.1186/s13321-022-00650-3

Wevers NR, Kasi DG, Gray T, et al., 2018. A perfused human blood–brain barrier on-a-chip for high-throughput assessment of barrier function and antibody transport. *Fluids Barriers CNS*, 15(1):23.

https://doi.org/10.1186/s12987-018-0108-3

Winklhofer S, De Martini IV, Nern C, et al., 2017. Dual-energy computed tomography in stroke imaging: Technical and clinical considerations of virtual noncontrast images for detection of the hyperdense artery sign. *J Comput Assist Tomogr*, 41(6):843-848.
https://doi.org/10.1097/rct.0000000000000638

Withnall M, Lindelöf E, Engkvist O, et al., 2020. Building attention and edge message passing neural networks for bioactivity and physical–chemical property prediction. *J Cheminforms*, 12(1):1.
https://doi.org/10.1186/s13321-019-0407-y

Wu D, Chen Q, Chen XJ, et al., 2023. The blood-brain barrier: Structure, regulation, and drug delivery. *Signal Transduct Target Ther*, 8(1):217.
https://doi.org/10.1038/s41392-023-01481-w

Xiong C, Yu Z, Yin Y, et al., 2025. Longitudinal changes of blood-brain barrier and transcytolemmal water exchange permeability in alzheimer's disease mice: A non-contrast mri study. *Neuroimage*, 310:121141.
https://doi.org/10.1016/j.neuroimage.2025.121141

Xu H, Li R, Duan Y, et al., 2017. Quantitative assessment on blood–brain barrier permeability of acute spontaneous intracerebral hemorrhage in basal ganglia: A ct perfusion study. *Neuroradiology*, 59(7):677-684.
https://doi.org/10.1007/s00234-017-1852-9

Yang G, Pan F, Parkhurst CN, et al., 2010. Thinned-skull cranial window technique for long-term imaging of the cortex in live mice. *Nat Protoc*, 5(2):201-208.
https://doi.org/10.1038/nprot.2009.222

Yang JY, Shin DS, Jeong M, et al., 2024. Evaluation of drug blood-brain-barrier permeability using a microfluidic chip. *Pharmaceutics*, 16(5):574.
https://doi.org/10.3390/pharmaceutics16050574

Yang XY, Wang QZ, Cao EH, 2020. Structure of the human cation-chloride cotransporter nkcc1 determined by single-particle electron cryo-microscopy. *Nat Commun*, 11(1):1016.
https://doi.org/10.1038/S41467-020-14790-3

Yin F, Su W, Wang L, et al., 2022. Microfluidic strategies for the blood-brain barrier construction and assessment. *TrAC Trends Anal Chem*, 155:116689.
https://doi.org/10.1016/j.trac.2022.116689

Yuan Y, Zheng F, Zhan CG, 2018. Improved prediction of blood–brain barrier permeability through machine learning with combined use of molecular property-based descriptors and fingerprints. *AAPS J,* 20(3):54.
https://doi.org/10.1208/s12248-018-0215-8

Zhang CE, Wong SM, Uiterwijk R, et al., 2019. Blood–brain barrier leakage in relation to white matter hyperintensity volume and cognition in small vessel disease and normal aging. *Brain Imaging Behav*, 13(2):389-395.
https://doi.org/10.1007/s11682-018-9855-7

Zhang H, Kang DH, Piantino M, et al., 2023. Rapid quantification of microvessels of three-dimensional blood–brain barrier model using optical coherence tomography and deep learning algorithm. *Biosensors,* 13(8):818.
https://doi.org/10.3390/bios13080818

Zhang S, Gong P, Zhang J, et al., 2020. Specific frequency electroacupuncture stimulation transiently enhances the permeability of the blood-brain barrier and induces tight junction changes. *Front Neurosci*, 14:582324.
https://doi.org/10.3389/fnins.2020.582324

Zhao Z, Nelson AR, Betsholtz C, et al., 2015. Establishment and dysfunction of the blood-brain barrier. *Cell*, 163(5):1064-1078.
https://doi.org/10.1016/j.cell.2015.10.067

Zhou J, Wilson DA, Ulatowski JA, et al., 2001. Two-compartment exchange model for perfusion quantification using arterial spin tagging. *J Cereb Blood Flow Metab*, 21(4):440-455.
https://doi.org/10.1097/00004647-200104000-00013